THESIS FOR THE DEGREE OF LICENTIATE OF ENGINEERING

# Development of a Yeast Model for Functional Analysis of Human Copper Transport Proteins

KUMARAVEL PONNANDAI SHANMUGAVEL


Department of Biology and Biological Engineering

CHALMERS UNIVERSITY OF TECHNOLOGY

Gothenburg, Sweden 2018

Development of a Yeast Model for Functional Analysis of Human Copper Transport Proteins

KUMARAVEL PONNANDAI SHANMUGAVEL



Department of Biology and Biological Engineering
Chalmers University of Technology
SE-412 96 Gothenburg
Sweden
Telephone +46 (0)31-772 1000

Cover Image:

Schematic Illustration of Yeast complementation.

# Development of a Yeast Model for Functional Analysis of Human Copper Transport Proteins

KUMARAVEL PONNANDAI SHANMUGAVEL

Department of Biology and Biological Engineering
Chalmers University of Technology

## ABSTRACT

Copper (Cu) is an important trace element that plays a vital role in several biological processes. It mediates numerous biochemical functions to maintain cellular homeostasis making it an essential metal for sustaining life. Many proteins or enzymes that are involved in various biochemical pathways require copper as a cofactor (also a regulator).

In human cells, the Cu uptake is mediated by high-affinity copper uptake protein (Ctr1), followed by cytoplasmic chaperone Atox1 that shuttles Cu from the plasma membrane to Wilson's disease protein ATP7B (P-type ATPase), a membrane-bound protein located at the Golgi apparatus. ATP7B incorporates Cu to various Cu-dependent enzymes in the secretory pathway. The main biological role of ATP7B (or Wilson Disease Protein) is to maintain the copper balance inside the human cell. Genetic defects in ATP7B often leads to a nonfunctional protein where copper balance is impaired and this condition results in Wilson's disease (WD). ATP7B is a large multi-domain membrane transport protein that shows typical characteristics of a P1b type ATPase. In contrast to its bacterial (CopA) or yeast (Ccc2) counterparts which have one or two metal binding domains (MBD) respectively, the human ATP7B has six cytosolic MBDs in the N-terminal region. The reason for the presence of these six MBDs in ATP7B is not completely understood, and neither is the ATP7B mediated copper release in the Golgi.

In this thesis, the development of a novel yeast model system for investigating the functional role of ATP7B in copper transport is described. The system probes shuttling of copper via human Atox1 to ATP7B proteins when expressed in a yeast humanized model. Using this system, we investigated the roles of six metal binding domains (MBDs) in ATP7B (Paper 1) and examined the Cu release (paper II). The results address the importance of the yeast model for studying human Cu transport proteins, the role of MBDs in ATP7B mediated Cu transport, the role of Atox1 in shuttling Cu and the significance of the luminal loop in ATP7B for Cu release function. Overall, the yeast model system developed in this thesis has great future potential for studying human copper transport proteins, which are involved in genetic diseases such as WD. The designed system can be expanded by using system biology approaches, to gain further understanding on human copper transport as well as copper transport related disorders.

**Keywords:** ATP7B, Wilson's disease protein, metal binding domains, luminal loop, yeast model, copper transport.

## LIST OF PUBLICATIONS

The licentiate thesis is written based on the following publications, referred to in the text by Roman numerals:

I. Probing functional roles of Wilson disease protein (ATP7B) copper-binding domains in yeast.
Kumaravel P Shanmugavel, Dina Petranovic and Pernilla Wittung-Stafshede
*Metallomics*, 2017 Jul 19;9(7):981-988.

II. A Lumenal loop of Wilson disease protein binds copper and is required for protein activity.
Birgit Köhn, Kumaravel P Shanmugavel, Min Wu, Michael Kovermann and Pernilla Wittung-Stafshede
*Biophysical Journal*, 2018, 115, 1-12

**CONTRIBUTION REPORT**

**Paper I.** I conceived the project together with PWS. Planned and performed all experiments and data analysis. I helped with writing the paper together with PWS.

**Paper II.** Planned and performed the yeast complementation and localization experiments, and analyzed the growth data.

## LIST OF FIGURES

## LIST OF ABBREVIATIONS

| | |
|---|---|
| AD | Alzheimer's disease |
| ALS | Amyloid lateral sclerosis |
| ATOX1 | Antioxidant-1 |
| BSA | Bovine serum albumin |
| CCS | Copper chaperone for superoxide dismutase |
| COX | Cytochrome c oxidase |
| CP | Ceruloplasmin |
| CryoEM | Cryogenic electron microscopy |
| CSM | Complete supplement mixture |
| DPPC | Dipalmitoyl phosphatidylcholine |
| DTT | Dithiothreitol |
| EDTA | Ethylenediaminetetraacetic acid |
| EGTA | Ethyleneglycol tetraacetic acid |
| EPR | Electron paramagnetic resonance |
| ER | Endoplasmic reticulum |
| HEPES | 4-(2-hydroxyethyl)-1-piperazineethanesulfonic acid |
| MBD | Metal binding domain |
| MD | Molecular dynamics |
| MES | 2-(n-morpholino)ethanesulfonic acid |
| MNK | Menke's disease |
| MT | Metallothionein |
| NBD | Nucleotide binding domain |
| NMR | Nuclear magnetic resonance |
| PAM | Peptidylglycine alpha-amidating monooxygenase |
| PD | Parkinson's disease |
| PVDF | Polyvinylidene difluoride |
| ROS | Reactive oxygen species |
| SD | Synthetic defined media |
| SDS | Sodium dodecyl sulfate |
| SOD | Superoxide dismutase |
| TGN | Trans-golgi network |
| TMD | Transmembrane domain |
| UV-Vis | Ultraviolet-visible |
| WD | Wilson's disease |

**TABLE OF CONTENTS**

## 1. INTRODUCTION

Biological systems are a complex networks of biochemical reactions and pathways, mediated by biomolecules. These systems require not just organic elements namely carbon (C), hydrogen (H), oxygen (O), nitrogen (N), phosphorous (P), and sulfur (S), but also various inorganic elements such as sodium (Na), potassium (K), calcium (Ca), and magnesium (Mg), so-called 'bulk elements'. On the contrary, elements such as cobalt (Co), copper (Cu), iron (Fe) and zinc (Zn) are required in traces and known as 'trace elements', which are essential for biological reactions. All these elements are required to maintain homeostasis, meaning the functional balance among different cellular components and pathways [1].

Metal ions are essential elements and play an important role in biological systems where they act as catalytic or structural cofactors of around one-third of all enzymes [2]. Transition metals notably Mn, Fe, Co, Cu, Zn, Mo, V and Ni are particularly important to maintain the structural integrity of the associated proteins [1]. Copper is involved in several key metabolic processes and is essential for life. In biochemical reactions, copper has important catalytic (i.e. oxidoreductases such as ascorbate oxidase, dopamine monooxygenase, galactose oxidase, and amine oxidase) and regulatory functions (proteins such as hephaestin, laccase, and zyklopen) that are needed for normal cellular growth, development, and overall physiological function. These roles require tight regulation of copper uptake in human cells [3].

Malfunction IN copper homeostasis lead to Menke's disease (Cu deficiency) and Wilson's disease (Cu accumulation)[4]. Wilson's disease (WD) is an autosomal recessive disorder of copper metabolism due to the mutations in the ATP7B gene. Normally, ATP7B is essential for the transport of Cu into the bile. However, any mutation in ATP7B can lead to a dysfunctional protein where Cu excretion by ATP7B into the bile is partly or completely hindered. Therefore, WD is often characterized by abnormal accumulation of Cu in the liver and brain cells. The frequency of the WD occurrence is 1 in 30000 individuals [5]. So far, more than 500 missense mutations have been identified in ATP7B with no known phenotype-genotype correlation [6]. Without any treatment, WD tends to be fatal due to serious liver failures and/or severe neurological disorders observed in most WD patients [7].

Moreover, intracellular copper accumulation in the cell can lead to many disturbances related to oxidative damage such as ROS generation, mitochondrial damage, dysregulation of lipid metabolism and apoptosis leading to cellular death at the final stage [4]. WD is mainly diagnosed using the knowledge based on clinical signs, histopathological findings, biochemical features and mutation analysis of ATP7B gene.

Until now direct genotype–phenotype correlations in WD have been difficult to identify because of the phenotypic variability in WD patients and animal models[7], which is one of the reasons why molecular mechanistic characterization and use of microbial models could be beneficial to advance this field.

In humans, the cellular uptake of copper is mainly regulated by copper transport protein Ctr1 ($Cu^{2+}$ reduction to $Cu^{1+}$) located on the cell membrane [8]. Further, the copper ($Cu^{1+}$) is taken up by the Cu chaperone Atox1 which shuttles Cu to Cu-ATPases (ATP7B and ATP7A) present in the Golgi apparatus. ATP7B then incorporates Cu to Cu-dependent enzymes such as ceruloplasmin (CP), lysyl oxidase, and tyrosinase present in the Golgi. At elevated intracellular Cu levels, the ATP7B is localized to the plasma membrane and acts as a Cu-exporter. The ATP7B protein is mainly responsible for maintaining Cu-homeostasis within the cell by loading Cu to Cu dependent enzymes in the Golgi or excreting excess Cu via entrapping into intracellular vesicles [9].

ATP7B (P1b type ATPase family) is a multi-domain protein that consists of eight transmembrane domains (TMDs) and three cytosolic domains namely: nucleotide binding domain (N-domain), phosphorylation domain (P-domain), and actuator/dephosphorylation domain (A-domain). The unique feature of ATP7B is the presence of six cytosolic MBDs in the N-terminal region. The six MBDs are connected by peptide linkers of various lengths. Similar Cu ATPase homologs in yeast and bacteria have only one or two MBDs[10]. The copper transport in ATP7B is mediated via ATP hydrolysis and a subsequent phosphorylation-dephosphorylation cascade where ATP7B is thought to undergo significant conformational changes through domain-domain interactions while Cu is moved across the protein [11]. The organization of the MBDs during the catalytic cycle is unknown due to limited structural information on the MBDs (i.e. arrangement of MBDs within full-length ATP7B is not known) [12]. To date, the high-resolution structural information of ATP7B (full-length ATP7B) has not been completely established (due to many different arrangements of the cytosolic domains in ATP7B). It has been hypothesized that Cu triggers conformation changes within the MBDs initiating the catalytic cycle subsequent to Atox1 mediated Cu delivery to the protein. It remains unclear if Cu is transferred via MBDs to the protein or Atox1 delivers it to the Cu binding site in the transmembrane domain directly like in the case of bacterial Cu ATPase, Cop A [13]. Moreover, there is limited information on how Cu is delivered to Cu dependent enzymes in Golgi. There has been very little focus toward studying the luminal side of ATP7B. It is speculated that Cu uptake by Cu dependent enzymes may happen via direct binding of Cu in the lumen, following the Cu release from ATP7B. In ATP7A (a P1B type-ATPase structurally similar to ATP7B), a protruding loop present in the lumen that connects transmembrane domain 1 and 2, has residues that can bind Cu and has also been suggested as the copper release site[14]. However, a clear proof for the presence of a similar release site is not present for ATP7B.

The general aim of this thesis is to describe the development of an engineered yeast system for investigating the role of MBDs and specific residues in ATP7B in copper transport. Previous yeast models that have been used to study Cu transport and as a diagnostic tool to determine the disease-causing mutations in ATP7B [15] do not regulate Atox1-ATP7B mediated Cu transport process. The model presented in this thesis is a new yeast system, which we used to assess the transport of Cu from human cytoplasmic Cu transport protein Atox1 to human Cu ATPase protein ATP7B in the yeast. For this purpose, we deleted yeast intracellular copper transport proteins Ccc2 and Atx1 and complemented these deletions with human copper transport proteins ATP7B and Atox1, which restored the wildtype phenotype. Further, the system was used to assess the functional roles of six MBDs in ATP7B in the presence of Atox1 (Paper I). In addition, we used this model to study the Cu binding residues in the luminal loop of ATP7B. Moreover, the *in vitro* NMR spectroscopy study was carried out for the identification of a potential Cu binding site in the ATP7B luminal loop (Paper II).

**Structure of the thesis**:

Following this brief introduction, **Chapter 2** establishes a theoretical background on main topics related to the presented research, along with a description of the methodologies used (**Chapter 3**). The original work of this thesis is summarized and discussed in **Chapter 4** which is based on the two appended papers (referred to as Paper I and II). Finally, a brief conclusion of the presented work in **Chapter 5** with an outlook about future directions of the research.

# 2. BACKGROUND

This chapter highlights an overview of the key topics, relevant to the work presented in the thesis. First, the biochemical properties and functions of copper are described, followed by copper homeostasis in prokaryotes and eukaryotes. Then, a brief introduction on dysregulation of copper homeostasis and its disorders. Further, the intracellular copper transport proteins in the human cell are explained with primary focus on ATP7B and Atox1 proteins. Finally, a detail introduction to the metal binding domains and the luminal loop of ATP7B is presented along with a description of the yeast complementation assay widely used in the work.

## 2.1 Functions of copper (Cu) in biological system

Copper is an element located in the group 11 in the periodic table of elements whose name derived from latin: *cuprum*, with atomic number 29, atomic weight 63.54, and electronic configuration: $3d^{10}4s^{1}$. Copper is a naturally occurring metal, which in an aqueous environment has the preferred oxidation state $Cu^{2+}$, and in a highly reducing environment (such as the cytosol) is reduced to $Cu^{1+}$ [16]. $Cu^{1+}$ is more favored than $Cu^{2+}$ in biological systems, since $Cu^{1+}$ more readily binds sulfur ligands such as cysteine, methionine or soft nitrogen ligands such as histidine. On the contrary, $Cu^{2+}$ binds hard nitrogen and oxygen ligands such as lysine, glutamine, and glutamate. The Cu binding sites of proteins are conserved across all organisms when compared to other trace metals. The reason for this conservation is that Cu is usually enzymatically active, and is required to undergo a functional valence change ($3d^{10}4s^{0}$ ($Cu^{1+}$) to $3d^{9}4s^{0}$ ($Cu^{2+}$), in aqueous environment) every turnover. To facilitate this, some Cu binding sites provide a ligand environment also known as entatic, meaning that Cu can be accommodated in an intermediate state between both preferred environments, thus allowing for an easy valence switch in between $Cu^{1+}$ and $Cu^{2+}$. The Cu binding sites are also classified as specific categories based on UV/VIS and EPR properties that are denoted as Type I (blue Cu, mononuclear, electron transfer, mainly cupredoxins, and Cu coordination sphere comprises of two imidazole nitrogens from histidine and one sulfur from cysteine), Type II (mononuclear, non-blue Cu, and Cu is mainly bound to imidazole nitrogens from histidine (3x histidine)) and Type III (dinuclear, EPR silent, and copper centers comprise of two spin-coupled copper ions, bound to imidazole nitrogens). Type II and Type III copper binding sites bind oxygen, and are mainly found in enzymes that function as oxidases or oxygenases [17].

Cu is involved in numerous biological processes such as the energy production, protein formation in the connective tissue, neuronal cell preservation, iron transport, phospholipid synthesis of cell membranes, antioxidant activity regulation of Cu-Superoxide dismutase (Cu-SOD), immune response elicitation against infection, contraction of heart muscle, cholesterol metabolism and development of blood vessels, skins and joints. These numerous functions of Cu in biological systems render it an essential component for human life. After iron, Cu is the second most desired transition metal ion (in terms of amount) for various organisms [18]. In addition to this, $Cu^{2+}$ forms the most stable complexes in accordance with the Irving-Williams series (relative stabilities of complexes formed by transition metals based on crystal field stabilization energy and ionic radius) [19]. Like all essential trace elements and nutrients, deficiency or overdose in the ingestion of Cu leads to decreased or increased Cu concentrations in the cells, each of which has its own unique adverse health effects. Humans have a complex homeostatic mechanism that maintains a constant supply of Cu and eliminates excess Cu [18].

Proteins that use Cu as a cofactor play diverse and vital roles in maintaining the metabolic and catalytic activity in the cell. Different Cu-binding proteins play different roles in this maintenance where amine oxidase is responsible for oxidizing primary amines, ceruloplasmin (multi-Cu oxidase in plasma) is essential for iron transport, cytochrome c oxidase (oxidase enzyme in the mitochondrial respiratory chain) is involved in the electron transport, Dopamine β-hydroxylase catalyzes the conversion of dopamine to norepinephrine which is involved in catecholamine metabolism, hephaestin: a multi-Cu ferroxidase responsible for the iron transport across intestinal mucosa into portal circulation, lysyl oxidase directs the cross-linking of collagen and elastin, Cu-SOD enzyme acts as defense against reactive oxygen species, and multi-functional enzyme peptidylglycine alpha-amidating mono-oxygenase (PAM) involves in maturation and modification of neuropeptides (i.e., neurotransmitters, neuroendocrine peptides), and tyrosinase catalyzes melanin and other pigment production [4].

In all reactions indicated above, copper is being utilized as a redox active metal to the benefit of the cell. However, copper is also a potent cellular toxin that is capable of catalyzing reduction or oxidation of other cellular proteins, membrane lipids and also DNA. Through Haber-Weiss reaction ($Cu^{1+}+H_2O_2+O_2^- \rightarrow Cu^{2+}+O_2+OH^-+OH^{\bullet}$), Cu is known to produce hydroxyl radicals (**.**OH) from hydrogen peroxide ($H_2O_2$) and superoxide ($O_2^-$) *in vitro. Invivo* production of these radicals can induce cellular damage by lipid peroxidation, DNA damage (strand breakage and base oxidation), protein damage and mitochondrial damage (reduced respiratory activity) [20].

The benefit of copper as a cofactor and the potential toxicity of copper make maintenance of Cu homeostasis a biological prerequisite for all living organisms [21], therefore any disturbance in this balance, especially in mammals leads to a set of metabolic diseases. A general overview of mammalian Cu homeostasis and disorders related to perturbation in this process will be discussed in the following section.

### 2.2 Copper homeostasis in humans

To ensure an optimal supply of Cu, the human body has a fine-tuned homeostatic system in which the Cu is absorbed, transported, distributed, stored and excreted. Several aspects of Cu homeostasis are known at the molecular level. An average of 70-80 mg of Cu is present in an adult human body. Each day around 0.5-2.5 mg of Cu is absorbed and an approximately same amount is excreted, thus a steady balance is maintained between dietary Cu absorption and its excretion[22].

Only about 50 % of Cu is absorbed from the ingested Cu and every day about 4.5 mg of Cu enters the portal circulation after being absorbed from the small intestine. The portal blood contains several Cu binding molecules such as transcuprein, albumin and small peptides helping Cu transport primarily to the liver where

the newly absorbed Cu are accumulated in the liver presumably via *transcuprein* or albumin within the first 2-6 hours. In the liver, Cu is then loaded to Cu-dependent proteins which are secreted into the blood. One of the major blood Cu carrier ceruloplasmin carries around 65 – 95% Cu excreted from the liver (Figure 1) and therefore most of the changes in blood plasma Cu levels are associated with the changes in serum ceruloplasmin concentration[23]. Bile is the main route of Cu excretion and is important in the regulation of cellular Cu levels and once the Cu is excreted to the bile, it cannot be reabsorbed (one-way route). Although major excretion occurs in the bile, relatively low amounts of Cu are delivered to the urinary tract. This makes liver the main homeostatic controller maintaining Cu levels in the body [24]. Within few hours of intestinal absorption, Cu levels in other organs such as kidneys and the brain tend to rise with the decrease in liver Cu levels[23]. Ceruloplasmin acts as a carrier for delivering Cu to these organs and also to other tissues[25].

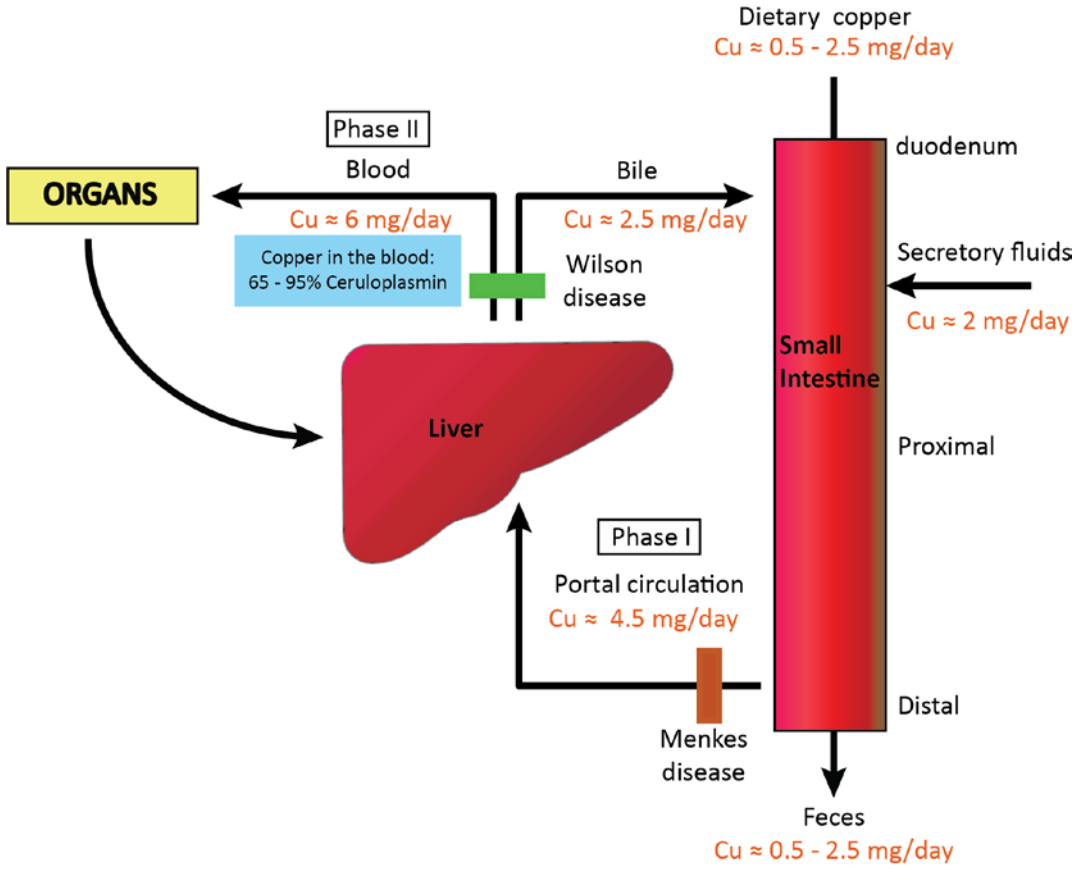


**Figure 1:** Overview of human Copper homeostasis

### 2.3 Copper transport in Human cells

The Ctr1 Cu transporter is responsible for the import of extracellular Cu across the plasma membrane in human cells. In humans, Cu induced endocytosis and degradation of the Ctr1 protein is used as means to regulate steady-state levels of Ctr1 at the plasma membrane. This regulation process is in contrast to yeast transcriptional regulation [26]. Until now, the Cu specific transcriptional control has not been identified in

mammalian cells. The Cu chaperones expressed in mammals are Atox1 (Atx1 homolog), Cox17 (cytochrome C oxidase Cu chaperone) and Ccs that delivers to ATP7A/B (Ccc2 homolog), Cox11 (protein involved in mitochondrial respiratory chain) and Sod1. Metallothioneins are also present in mammalian cells, but their regulation by transcription factor MTF1 is mediated in indirect manner (i.e. by liberating bound zinc from MTF1) [20, 27]. After Ctr1-mediated Cu uptake in the intestinal cells, the Atox1 shuttles Cu to ATP7A at the basolateral membrane where ATP7A pump Cu into the portal circulation (blood). In other cells, ATP7A shuttles between the Golgi apparatus and the cell membrane to maintain Cu homeostasis and provides Cu to Cu dependent enzymes present in the Golgi apparatus.

The major Cu storage organ is the liver which takes up Cu from the portal circulation. ATP7A is expressed in many tissues except the liver, where its expression diminishes during maturation. In liver and other tissues, the main Cu transporter is ATP7B which delivers Cu to cuproenzymes such as ceruloplasmin, peptidyl monooxygenase, tyrosinase, and lysyl oxidase in Golgi apparatus, in a similar manner like ATP7A. ATP7B mobilizes excess Cu into the bile to prevent Cu overload (Figure 2) [22]. Ceruloplasmin (ferroxidase, plasma protein) is the major Cu-carrying protein in the blood and in addition plays a vital role in iron metabolism [28]. Cu deficiency in mice due to defective Ctr1, induced an unknown signal that stimulates the activation of intestinal ATP7A expression. Unlike yeast, the transcriptional regulation of Cu proteins in mammals is not well known.

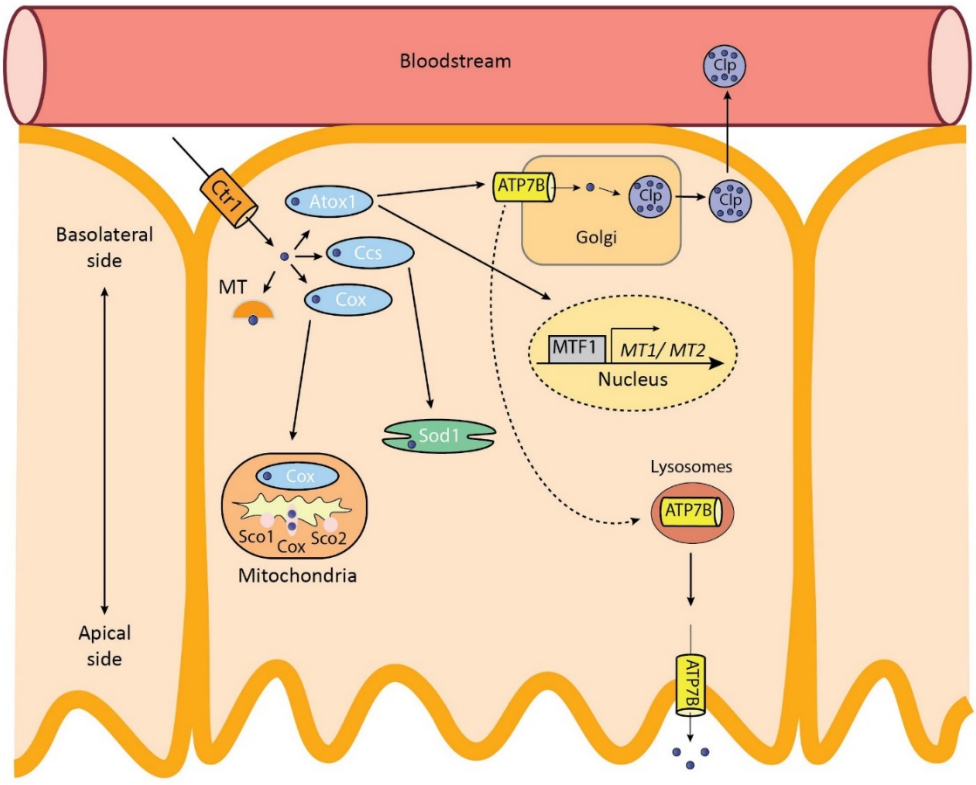


**Figure 2:** Schematic representation of proteins involved in copper transport in mammalian cells. (Adapted from 'Copper: An essential metal in biology' by R. Festa and D. Thiele, *Current Biology*, 2011, 21(21): R877–R883).

## 2.4 Copper transport in Yeast

There is an array of metalloproteins that exist in single-celled eukaryotes that are located within organelles such as mitochondria, chloroplast, and secretory compartments. The copper homeostatic mechanism was first described in *Saccharomyces cerevisiae* (*S. cerevisiae*), a more complex organism as compared to the prokaryotic counterparts. The Cu import in *S. cerevisiae* is dependent on two functionally redundant high-affinity membrane Cu transporters; Ctr1 and Ctr3 (similar function to Ctr1)[29] and a low-affinity transporter Fet4, in which Cu is transported subsequently to the reduction from $Cu^{2+}$ to $Cu^{1+}$ by Fre1, a Cu-reductase located on the plasma membrane [26]. However, the majority of Cu imported is via Ctr1 and Ctr3 under low Cu conditions where Ctr1, Ctr3, and Fre1 are activated via the translational regulator MAC1. At elevated Cu levels, endocytosis and degradation of Ctr1 are promoted [20, 30].

Under basal conditions, cytoplasmic Cu chaperones Atx1 and Ccs (copper chaperone for superoxide dismutase) receives Cu from Ctr1 or Ctr3 and shuttles it to other Cu dependent proteins present in the organelles. Briefly, Atx1 delivers Cu to Cu-binding protein Ccc2 (P-type ATPases) localized at the trans-Golgi network which then loads Cu to the Fet3, a Cu-dependent multi-copper oxidase [20]. Another route for Cu is through Cu/Zn superoxide dismutase Sod1 that localizes both in cytoplasm and mitochondria and the Cu is received from Cu chaperone Ccs which has a similar domain structure (domain II) to Cu binding domain of Sod1. Sod1 is crucial for detoxification of highly toxic superoxide radicals ($.O_2^-$) and hence a great protection from the emerged oxidative stress. In case of low external Cu, *S. cerevisiae* responds to the Cu shortage by using the pre-stored Cu within the vacuole, via a process carried out by Ctr2 and a vacuolar localized metalloreductases, Fre6 [31].The mitochondria are also used as a Cu-storage pool under low Cu conditions and accommodate a Cu-dependent enzyme, Cytochrome c oxidase, which uses Cu for maintaining an optimal activity. During this process, several mitochondrial-associated proteins such as Cox17 (cytochrome C oxidase), Sco1, and Sco2 (Sco 1and 2 cytochrome C oxidase assembly protein) are involved in the delivery of Cu to cytochrome c oxidase[26].

Apart from its uptake and distribution, a detoxification process is essential to encounter an increase in environmental Cu. This process is carried out by metallothioneins (Cup1, crs5), a group of protein that scavenges excess Cu from cells. Metallothioneins have a tight Cu-coordination through cysteine thiolates, making Cu poorly exchangeable and not highly reactive. Metallothioneins were initially thought to be present only in eukaryotes but *Mycobacterium* and *Synechococcus* species also contain these proteins [26]. *S.cerevisiae* activates distinct genes in responses to low and high Cu using specific Cu-sensing transcription factors. Under high Cu concentrations, transcription of Cup1, Crs5, and Sod1 genes are activated by transcription regulator ACE1[20]. A pictorial illustration of copper transport process in eukaryotes is shown in Figure 3.

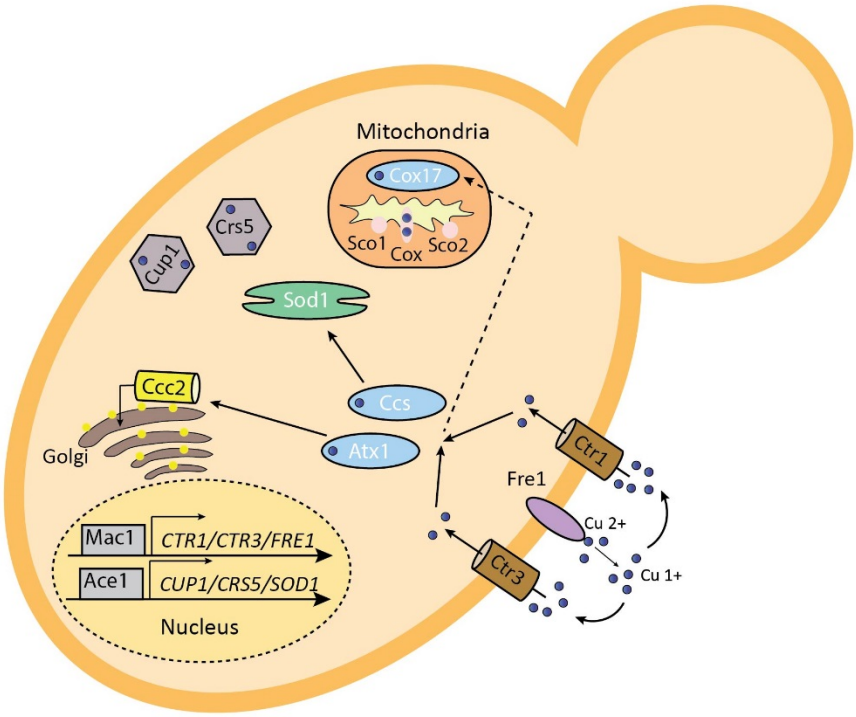


**Figure 3:** Illustration of copper transport process in single cell eukaryotes. (Adapted from 'Copper: An essential metal in biology' by R. Festa and D. Thiele, *Current Biology*, 2011, 21(21): R877–R883).

### 2.5 Crossroad of Copper and Iron transport in yeast

As described above, the Cu-transport in yeast is well regulated. The Cu is generally taken up by yeast cell as free ion form not complexed to any ligands. The Cu is reduced to Cu(I) by plasma membrane reductase proteins Fre1 and Fre2, prior to uptake. Cu transport is largely reduced in absence of reductase proteins but this can be reversed by addition of chemically reducing ascorbate. The reduction is the main step in Cu uptake process. Ctr1 (a 190 aa, homotrimer) is a high-affinity Cu transporter, localized in the plasma membrane is responsible for Cu uptake. Ctr1 has 3 membrane-spanning helices and a N-terminal domain (ectodomain, 67aa) containing 11 repeats of histidine and methionine rich motif which is predicted to bind Cu [8].The mechanism of Ctr1 mediated Cu transport is difficult to determine since it does not share sequence similarity with known Cu transport proteins. The cytosolic Cu chaperone Atx1 delivers Cu to Ccc2 which is localized in the TGN. In the post-Golgi vesicular compartment, Cu is incorporated to cuproenzyme Fet3 by Ccc2. Fet3 is responsible for high-affinity iron uptake in yeast. The main function of Fet3 is to catalyze the oxidation of $Fe^{2+}$ to $Fe^{3+}$ (ferroxidase reaction) using oxygen as substrate[32]. Binding of Cu to Fet3 initiates the oxidase activity, as no oxidase activity is present in apo-Fet3. Cell surface-localized Fet3 together with iron permease Ftr1 mediates high-affinity iron uptake. The oxidase function of Fet3 is required at the plasma membrane for iron uptake. The $Fe^{3+}$ generated by Fet3 is a ligand for the iron permease Ftr1 which uptake extracellular iron [33]. Ccc2 protein connects the Cu uptake pathway to iron uptake pathway in yeast (Figure 4). The high-affinity iron uptake pathway is dependent on Cu transport in yeast and the iron uptake pathway (Fre1, Fre2, Atx1, Ccc2, Fet3, and Ftr1) are regulated by the transcription factor AFT1 during iron starvation.

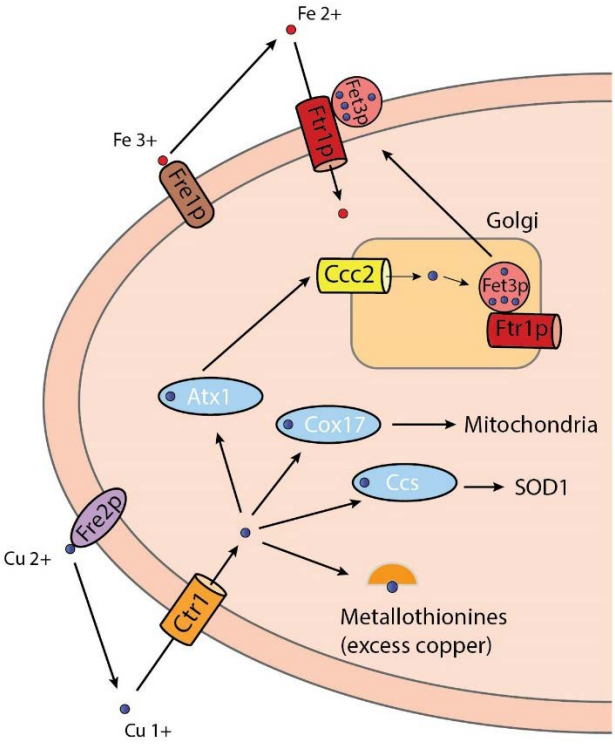


**Figure 4:** Yeast copper and iron homeostasis. Copper transport in yeast cells is closely linked to the iron transport. Ccc2 delivers Cu to Fet3 enzyme in the Golgi apparatus which is also coupled to iron import by Ftr1. Fre1 and Fre2, as two membrane-bound metalloreductases is also responsible for reduction of Fe as well as of Cu. (Adapted from 'Copper and copper containing pesticides: metabolism, toxicity and oxidative stress' by V. Husak, *JPNU*, 2015, 2(1): 38–50).

### 2.6 Role of Cu in human diseases

The Cu uptake, distribution, and export processes are fundamentally essential to maintain Cu homeostasis in any cell. Any perturbation to this process leads to Cu overload or Cu deficiency which have distinct critical effects on cellular function. Excess Cu intake, in turn, induces toxicity by interacting with other nutrients, and Cu deficiency disturbs the iron transport and metabolism which results in anemia [34] due to decreased iron concentration in blood. On the other hand, Cu toxicity induces oxidative damage in the cells which results in DNA damage, peroxidation of lipids and mitochondrial damage [9]. Cu-related metabolic diseases are discussed in this section:

#### Wilson's Disease (WD)

Wilson's disease (WD) is a rare autosomal recessive genetic disorder of Cu transport and is caused by abnormal accumulation of Cu in the liver due to an inactive P1B-type ATPase; ATP7B. Under normal conditions, this protein is responsible for transporting Cu from the liver to bile for excretion. However, certain mutations in the ATP7B gene leads to dysfunction of Cu transport and hence the poor incorporation of Cu into ceruloplasmin as well as an impaired biliary Cu excretion leading to toxicosis (Cu accumulation) in the liver, brain, kidneys, eyes and other organs)[35].

Approximately 1 in every 30 000 individual is affected by Wilson Disease and the onset is in the range of 3-50 years of age. Its widespread symptoms include hepatic disorder, neurological problems, skeletal and rarely renal or endocrine problems[7]. If untreated, the progression of this disease has adverse effects such as the development of encephalopathy and kayser-fleischer rings (discoloration at the outer rim of iris due to Cu accumulation). Early diagnosis and treatment can allow a patient to live a long and healthy life. The treatment for this disorder is Cu chelators (D-pencillamine, Zinc sulfate/acetate) which bind Cu and enables patients to excrete excess Cu [36].

The disease-causing mutations of ATP7B are missense, frameshift, non-sense or splice-site mutations [37]. These mutations can hinder every step of the catalytic cycle of ATP7B, which is the main regulator of Cu transport [11]. The most common WD mutations are observed in the conserved regions of the ATPase core (transmembrane domain) [38], but some mutations are also observed in other parts of ATP7B (i.e. A-domain, MBDs). The most common WD mutations are R778L, H1069Q, and R778W. The R778L (58% of all WD mutations) mutation is located in the TMD4 (lies close to A-domain) and this specific mutation is observed in patients of southeastern Asian countries (Korean and Chinese patients). The H1069Q (around 35-45% of all WD mutations) mutation is found in the N-domain and mostly prevalent among European descent (Europer and North America). The R778W mutation is common among Indian population [39].

**Menke's Disease (MNK)**

Menke's disease (MNK) was first identified by John Menkes in1962. This is a genetic disease that is mainly caused by a non-functional Cu transporting ATP7A (responsible for Cu efflux from intestinal cells into blood) and hence results in Cu deficiency. It is a rare X-linked disorder that affects 1 in 200 000 people worldwide. ATP7A is mainly located on the luminal side of human intestinal epithelial cells and is responsible for transporting Cu from intestine to different organs and tissues. Mutational defects in ATP7A cause Cu to remain trapped within the lining of the small intestine and hence all Cu transport to the liver, blood and other organs are disrupted. Symptoms associated with this disease are usually observed with coarse, brittle, depigmented hair, mental retardation, skeletal defects, abnormal connective tissue growth and inability to control body temperature [40]. Patients with Menke's disease suffer from severe neurological abnormalities owing to the lack of cuproenzymes required for brain function and development as well as with a decrease in the Cytochrome c oxidase activity. The cause of hypopigmentation of hair and brittle steely appearance is not yet known, but is thought to be the loss of an unidentified cuproenzyme. Defective collagen, elastin polymerization and connective tissue abnormalities (loose skin, fragile bones, aortic aneurisms) are thought to be in connection with a reduced enzymatic activity of lysyl oxidase[41]. This disease is usually fatal even with the early diagnosis and its treatment is carried out by both intraperitoneal and intrathecal Cu histidine administration to the central nervous system to prevent severe neurological problems.

**Aceruloplasminemia**

Ceruloplasmin (CP) is a serum plasma protein which carries upto 95% of Cu present in the blood plasma. Ceruloplasmin is a multi-copper oxidase, which during biosynthesis starts as an apo-protein that is loaded with six Cu atoms (Figure 5) by ATP7B in the Golgi. These Cu atoms provide stability to the CP protein [42]. The bioavailability of Cu does not affect CP , but the apo-form of CP is rapidly degraded in the plasma showing that Cu is essential for the protein to thrive and to perform its function [43]. The main role of the ceruloplasmin in the serum arises from its ferroxidase activity and its ability to carry Cu in the blood. The ferroxidase reaction (oxidation of $Fe^{2+}$ to $Fe^{3+}$, reduction of $Cu^{2+}$) involves the oxidation of iron

(Fe) before its incorporation into plasma transferrin (a protein that transports Fe to red blood cells to carry oxygen). This makes Cu-carrying ceruloplasmin essential for iron efflux from cells [44].

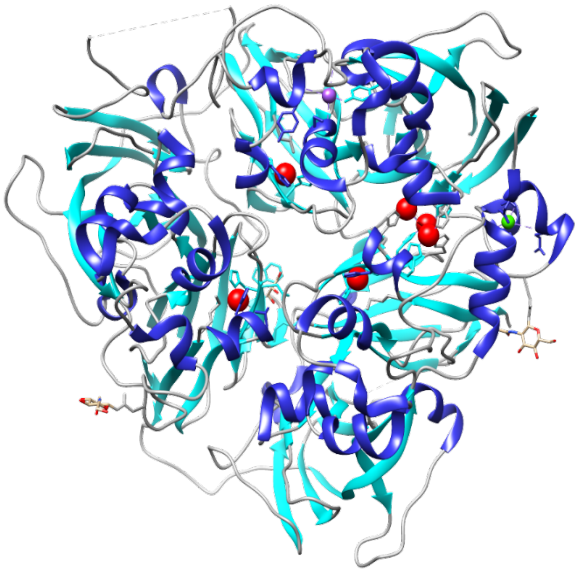

**Figure 5:** Secondary Structure illustration of human multi-copper oxidase ceruloplasmin. (crystal structure of holo-ceruloplasmin, Pdb:4ENZ, Cu ions are shown in red spheres)

Aceruloplasminemia is observed via the gradual accumulation of the iron in the retina, basal ganglia, and other organs. Iron accumulation in the brain causes neurological problems such as dystonia, dysarthria, and subcortical dementia. This disease is a rare autosomal recessive disorder and genetic studies have shown the cause of the disease is to be due to the mutations of the ceruloplasmin gene. These mutations in CP makes it incapable to mobilize iron out of the tissues (due to reduced Cu binding to CP which in turn affects Fe transport and oxidation of substrates such as primary amines) and incorporate iron into transferrin [45] resulting in Fe accumulation in hepatic and reticuloendothelial cells. Although these tissues have remarkably high levels of iron accumulation, their Cu levels are normal in all patients.

**Amyloid Lateral Sclerosis (ALS) / Lou Gehrig disease**

This is a neurodegenerative disease that affects the upper and lower motor neurons leading to progressive muscle weakness, atrophy and ultimately results in death within three years from onset of the disease. ALS is either sporadic (1-2%) or familial (10-20%) (genetically inherent), autosomal dominant disorder which is caused by a missense mutation in the SOD1 gene (discovered in 1993). This mutation makes SOD1 gain an increased activity, unlike other diseases described in this section which are caused by the lowered activities of related proteins [46]. The disease is also caused by mutations in the C9ORF72 gene (discovered in 2011, 25-40% of all familial ALS), the NEK1 gene (discovered in 2016, 3% of all ALS), the TDP43 (discovered in 2008, 4% familial, and 1% sporadic), and other ALS genes such as FUS, UBQLN2, KIF5, and VCP [47, 48]

Sod 1 is a highly conserved enzyme with a homodimer structure containing one Cu ($Cu^{2+}$) and one zinc ($Zn^{2+}$) per subunit. It catalyzes the disproportionation of superoxide anions ($O_2^{\cdot-}$) to hydrogen peroxide ($H_2O_2$) and oxygen ($O_2$) via cyclic reduction and oxidation of bound Cu ions. Mostly, gain of function mutations (missense mutations) occur outside the enzymatic active site forming a cluster in loops of joined β-barrel structures. As a result, the stability of the enzyme is altered leading to an increased turnover of Sod1 with the reduction of zinc binding and an increased formation of aggregates [49]. The holo-mutant Sod1 (Cu-bound mutant Sod1) enhances the production of free radicals and accumulation of Sod1 aggregates in cells, especially in motor neurons. Therefore, ALS patients are treated with Cu-chelators (Penicillamine, ammonium tetrathiomolybdate) to prevent the abnormal production of free radicals as well as caspase-induced apoptosis [50].

**Copper in Alzheimer's disease (AD)**

Alzheimer's disease (AD) is a neurodegenerative disorder that causes dementia. The development of familial and sporadic forms of this disease involve accumulation the of amyloid beta protein. Aβ is derived from the transmembrane amyloid precursor protein (APP) and mutation in this protein results in familial AD [51]. The Aβ aggregates perturb the cellular ion homeostasis and induce cellular oxidative stress. Under mild acidic conditions (pH 6.5-6.8), Cu ($Cu^{2+}$) promotes the aggregation of Aβ *in vitro* [52]. The APP protein binds $Cu^{2+}$ and reduces it [53]. The reduced Cu remains bound as the APP protein is delivered from the cell body to axonal cell surface and dendritic plasma membrane [54]. The transcellular transport of Cu by APP disrupts the normal Cu transport in the cell [49, 55]. In presence of hydrogen peroxide, the bound Cu is re-oxidized and is accompanied by fragmentation of APP to distinct aggregating peptides.

**Copper in Parkinson's disease (PD)**

Parkinson's disease is associated with aggregation of the intrinsically disordered alpha-synuclein protein. Parkinson's disease patients have dysregulation of Cu homeostasis, decreased expression of Ctr1 and reduced tissue Cu levels in the *substantia nigra [56]*. The alpha-synuclein protein tends to have high-affinity towards $Cu^{2+}$ and their interaction leads to the production of toxic oligomers (which damage the cell membrane) [57] and induction of oxidative stress via ROS production [58]. Specifically, alpha-synuclein (H50Q) mutation tends to promote fibrillation in presence of $Cu^{2+}$ which is postulated to cause severe neuronal damage [57]. Cu dyshomeostasis in PD patients is related to genetic mutations (A1135Q) of ATP7B [46, 49].

**Copper in Human Prion disease**

Human prion disease is caused by the accumulation of the post-translationally modified form ($PrP^{Sc}$) of the normal cellular prion protein ($PrP^{C}$). Binding of $Cu^{2+}$ to the amino terminus (octapeptide in N-terminus of $PrP^{C}$) of prion protein induces misfolding and aggregation due to conformational changes. $Cu^{2+}$ binding alters the structure from α helical to β sheets, this conformational shift provides resistance against protease digestion [59]. Recent studies provided evidence that prion protein might play a role in Cu homeostasis [55] by receiving Cu from the plasma membrane and delivering it to target proteins. Certain studies suggest that PrP is a cuproprotein and regulates Cu bioavailability in cells [46].

### Copper in Cancer

Cancer is a complex disease with various causes and this makes it difficult to know the defined mechanism by which the tumors are initiated and propagated[60]. However, Cu is found to promote tumor growth [61]. The tumor cells contain elevated levels of Cu in comparison with normal cells. Therefore, Cu chelators are being used in the treatment of cancers[62]. Once Cu chelators are administered, Cu-chelator complexes are formed inside tumor cells, these complexes are toxic and induce tumor cell death (via oxidative stress) [61, 62]. Since normal cells have low Cu levels, administration of these agents does not cause cell death for healthy cells [63].

## 2.6 Intracellular Cu transport proteins

### Copper chaperone Atox1

Antioxidant -1 (Atox1 or Hah1 cytosolic human Cu chaperone) was identified as a chaperone due to its similarity with Atx1 (the fungal Cu chaperone). Atox1 has ferredoxin-like fold (βαββαβ) (Figure 6) and Cu binding motif (MXCXXC) similar to Cu binding motif of MBD in ATP7B[64, 65]. The Cu binding motif is located within the loop that connects the first β-strand and the following first α-helix. This motif has a strong affinity for Cu (I). Cu binding increases the chemical and thermal stability of Atox1 and known to increase the overall stability [66]. The Cu(I) that is imported by Ctr1 is bound by Atox1, which then shuttles it to metal binding domains of ATP7A and/or ATP7B. This delivery of Cu to MBDs are confirmed by *in vitro* studies [67]. Atox1 can deliver Cu(I) to all MBDs *in vitro* but not all MBDs are equivalent in receiving Cu. The MBD1, MBD2, and MBD4 are known to form Cu(I)-bridged adducts with Atox1 whereas the adduct formation was not observed for MBD3, MBD5 and MBD6 but there is still Atox1-mediated Cu transport [12].

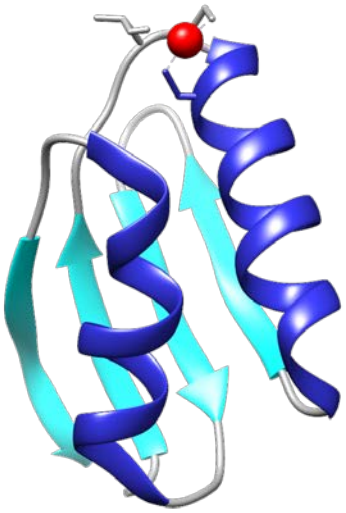

**Figure 6:** Secondary Structure illustration of human Cu chaperone Atox1 (Solution structure of holo-Atox1, Pdb: 1TL4, Cu ions are shown in red spheres). Copper binds the loop (MXCXXC motif) connecting first β strand and first α helix.

Atox1 plays a vital role in Cu homeostasis. Apart from this, Atox1 is predicted to have numerous functions in the cell that have yet to be elucidated [68]. Like conserved Cu binding motif, there are other amino acids in Atox1 which are also conserved. The conservation of lysine-rich KKTGK amino acid residues (conserved in Atx1) located between the second α-helix and the last β-strand may indicate it to be a nuclear localization signal [69]. The Lys60 residue is also conserved and was shown to be important for Cu delivery. In Atx1, the Lys60 is known to be essential for antioxidant activity and Cu delivery [70]. The ATOX1 knockout cells displayed reduced Cu ATPase activity, and the ATOX1 deficient animals exhibited growth failure [71].

**P-type ATPase: ATP7B**

The P-type ATPases (or E1-E2 ATPases) are a group of proteins that function as ion pumps that are found in bacteria, archaea, and eukaryotes. They are all varied depending upon the physiological process in humans that they are involved in. The Sodium–potassium pump, proton-potassium pump, calcium pump and plasma membrane proton pump of plants and fungi are prominent examples of P-type ATPases (heavy and non-heavy metal ATPases) [72]. The heavy metal ATPases form a distinct subgroup of P-type ATPase termed as CPx type ATPase [73].

The P-type ATPase transporter family usually functions as a cation uptake or efflux transporter, but certain proteins in this family are also involved in flipping phospholipids to maintain the asymmetric nature of the biomembrane [74]. The unique feature of P-type ATPases is the auto-phosphorylation of a conserved aspartate (D) residue by ATP hydrolysis (energy source) for driving the ion transport. During the transport process, the transporter have a tendency to interconvert between at least two different conformations (open, E1 and closed, E2 states,[11]) after being bound with the inorganic phosphate (Pi) and the ion to be transported in. P-type ATPases have a single catalytic subunit that hydrolyzes ATP (via N-domain and A-domain), contain an aspartyl phosphorylation site (P-domain), the binding site for the metal ion and catalyzes ion transport. The catalytic subunit is composed of a cytoplasmic section that consists of a phosphorylation domain (P-domain), nucleotide binding domain (N-domain), actuator domain (A-domain) and a transmembrane segment (TMDs) with the binding site for the metal ion. The cytoplasmic section contains over half the mass of the protein. Some family of P-type ATPases have additional subunits for their function or accommodate additional regulatory domains [75]. The P1b-type pumps have several N- and C-terminal heavy metal binding domains (also cytoplasmic) which have a role in the catalytic activity regulation of the protein [72].

**CPx type ATPases**

CPx type ATPases belong to a subgroup of P-type ATPases, which have the unique feature of a conserved intramembranous cysteine-proline-cysteine or cysteine-proline-histidine motif. The novel features of CPx type ATPases are 1) putative metal binding sites in the polar amino-terminal regions, 2) a conserved intramembranous CPC, CPH or CPS motif, 3) a conserved histidine –proline dipeptide (HP locus) 34 to 43 amino acids C-terminal to the CPx motif, and 4) a unique number and topology of the membrane-spanning domains. The CPx motif is generally present in the $6^{th}$ transmembrane domain and this region is termed as ion transduction domain or ion channel. The amino acids surrounding the proline residue vary with ion specificity of the transporter. The intramembranous CPC or CPx motif is a distinguishable feature of heavy metal pumping ATPases. The Histidine – Proline locus is present in all CPx type heavy metal ATPases but not in non-heavy metal ATPases. Mutation of histidine present in the HP locus of ATP7B (H1069Q) makes the protein non-functional thus causing abnormalities in Cu homeostasis[73].

**ATP7B**

Wilson's disease protein ATP7B (CPx type ATPase) is a Cu transporting P-type ATPases and is primarily expressed in the liver and kidneys, but is also detected at lower levels in lung, placenta and brain [76]. ATP7B helps in maintaining Cu levels in the body by excreting excess Cu into the bile and plasma. The genetic defect in ATP7B mostly leads to dysfunctional ATP7B that cause Cu accumulation in tissues leading to neurological, psychiatric issues and liver diseases [77]. ATP7B is located on chromosome 13 and comprises 21 exons that span an approximate size of 80 kb. The transcribed mRNA size is around 7.5kb, which contains coding regions of 4.5 kb that translates to a 165 kDa (1465 amino acid) protein [35]. The ATP7B protein delivers Cu to the Cu-dependent enzymes in the trans-Golgi network. The Cu-dependent enzymes such as ceruloplasmin, tyrosinase, lysyl oxidase, and blood-clotting factors, which are transported via the secretory pathway depend on ATP7B for Cu delivery. At elevated intracellular Cu levels, the ATP7B protein acts as a Cu exporter to maintain Cu homeostasis[78]. Alternate splicing of ATP7B transcript generates different isoforms with distinct cellular localization. The ATP7B present in the brain cells (140 kDa) is smaller in size than in the hepatocytes[79].

ATP7B is a multi-domain protein with a cytosolic region composed of actuator domain (A-), phosphorylation domain (P-), nucleotide binding domain (N-), six metal binding domains (MBDs), and has eight membrane-spanning domains (TMDs) (Figure 7).The cytoplasmic N-terminal part of the protein has six metal binding domains that are connected together in a linear chain by short flexible linkers [80]. In vitro studies on MBDs of ATP7B have demonstrated that MBDs receive Cu from Cu chaperone ATOX1 [67]. The metal binding domains consist of the consensus motif of MXCXXC that displays the Cu binding site. The Cu chaperone Atox1 has the same consensus motif that binds Cu (in Atox1: Cu (I) is coordinated in a distorted linear geometry to sulfurs of cysteine to form a bond angle of 120°) and has a similar structure to that of metal binding domains of ATP7B [67]. A TGN retention signal is present in the amino terminus of ATP7B. The eight transmembrane segments are anchored in the Golgi membrane and have an appearance of a helical bundle. Adjacent transmembrane domains are connected by a loop segment [81]. The CPC motif in the transmembrane segment (ion transduction domain) is characterized as a Cu binding site. The protein uses ATP hydrolysis to move Cu. ATP binding to the ATP binding domain initiates the Cu transport and Cu binds to the transmembrane region. Further, phosphorylation occurs at the aspartic residue in the DKTGT motif in the phosphorylation domain with Cu release. After this, the dephosphorylation of the aspartic acid residue converts the protein back to the initial conformation for the next transport[34]. A cryo-EM structure was recently established that shows ATP7B forms dimers (Figure 8A&B). For ATP7B dimerization, the contact between phosphorylation and ATP binding domain and transmembrane contacts are responsible[82].

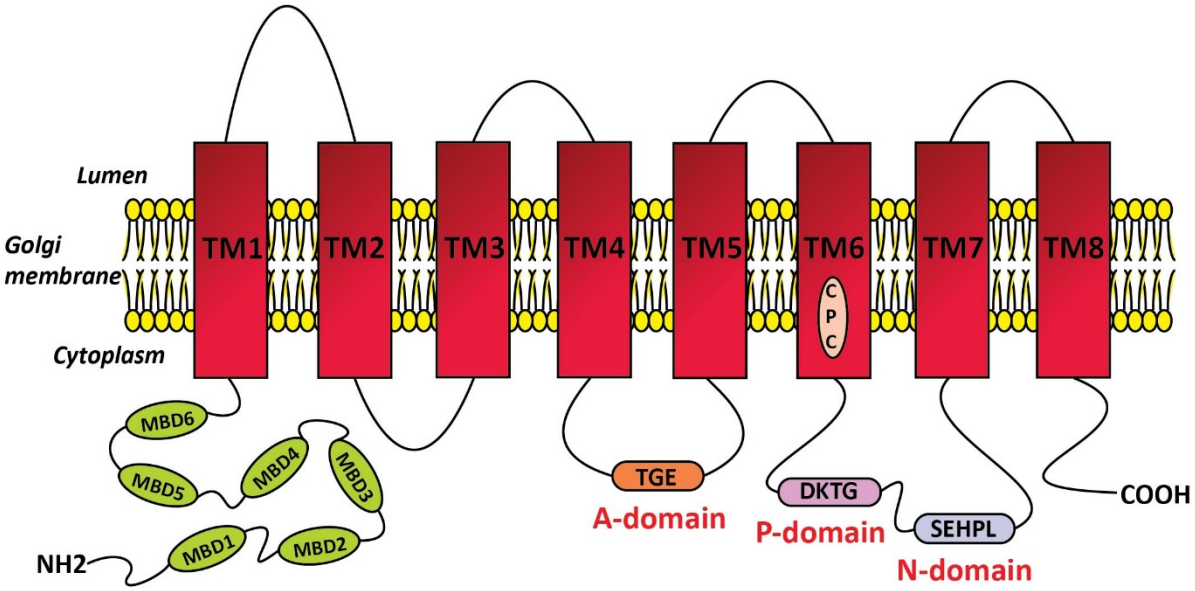


**Figure 7:** Structural organization of ATP7B. Characteristic functional domains of Cu-P1B type ATPase is illustrated for ATP7B which consists of eight transmembrane domains; TMDs (red), six metal binding domains; MBDs (green), dephosphorylation domain; A-domain (orange), phosphorylation domain; P-domain (pink) and nucleotide binding domain; N-domain(blue, HP locus is present in this region). A combination of N- and P- domain are usually referred as ATP-binding domain.

The post-translation modification of ATP7B in humans generates a long and a short variant of ATP7B. The short variant is localized in the cytosol (cytoplasmic membrane vesicles) of brain cells whereas the long variant is the most common form, and is localized in the Golgi membrane (TGN) of hepatocytes [79]. The localization of ATP7B on the TGN was identified using immuno-histochemical methods [83]. The localization of ATP7B changes with respect to intracellular Cu levels. In high intracellular Cu conditions, the TGN localized ATP7B exits the Golgi and enters the cytoplasmic membrane vesicles (intracellular ATP7B trafficking is partly known to depend on MBDs and certain residues in first transmembrane segment [84]). Later, the vesicle containing ATP7B is translocated to the apical membrane, for exporting Cu in the process known as apical trafficking [85]. The predominant changes in ATP7B localization help to maintain Cu homeostasis [86]. Apart from the intracellular Cu levels, the specific disease-causing mutation in ATP7B also affects the localization of ATP7B protein. ATP7B with Arg877Leu and His1069Glu mutations are localized in the endoplasmic reticulum and Asp765Asn /Leu776Val mutation affects the localization of ATP7B on the TGN. Certain mutations in ATP7B do not affect the TGN localization, but disrupt Cu transport [87]. Deletion of domains in ATP7B also affect the TGN localization. In addition, misfolding of ATP7B protein causes it to localize in the ER. Certain ATP7B mutations and domain deletions appear to destabilize the protein, as a result, the protein localizes to the ER. These localization problems were overcome by treatment with pharmacological chaperones such as phenylbutyrate (4-BPA) or curcumin that rescue the protein variants back to TGN [88].

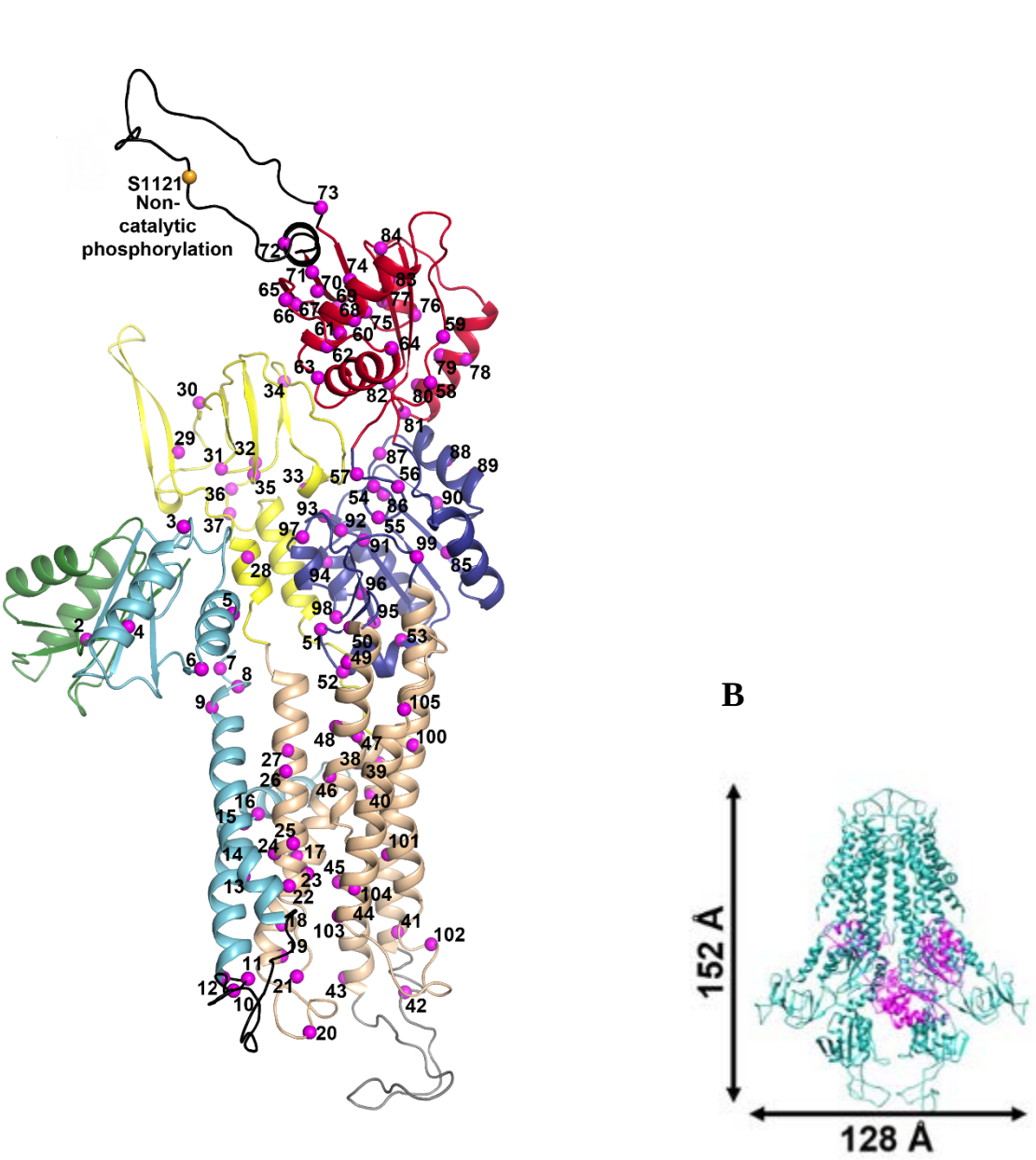


**Figure 8:** Three dimensional model of ATP7B (**A**) Homology model of ATP7B (1-4Δ MBD). The TMD (helices) are connected to MBD6 (cyan). MBD5(green), A-domain(yellow), P-domain(blue), and N-domain(red). Magenta spheres indicate missense WD mutations (Reprinted from 'Structure models of the human copper P-type ATPases ATP7A and ATP7B' by Gourdon et al, *Biological chemistry*, 2012, 393(4): 205–216). (**B**) Dimer model of ATP7B (1-4Δ MBD, dimer interface P-N domain). MBD5, and 6(magenta) (Reprinted from 'Human copper transporter ATP7B (Wilson disease protein) forms stable dimers *in vitro* and in cells' by Jayakanthan et al, *Journal of Biological chemistry*, 2017, 292 (46): 18760–18774).

ATP7B also functions as a Cu efflux transporter in the plasma membrane besides the role of Cu delivery to enzymes in Golgi [83]. In dendritic and somatic cells, during basal $Cu^{2+}$ conditions, most of the ATP7B

protein is localized to the plasma membrane, rather than the TGN [89]. Numerous studies on Wilson's disease models has also highlighted the localization of ATP7B to the plasma membrane [24] [6]. The ATP7B expression in human breast epithelial cells directs to the apical membrane to expel Cu under elevated levels but in the case of deletion or mutation in N –terminal metal binding domains the ATP7B is trafficked to the basolateral membrane [90] [91]. Cell-membrane localization is affected by mutations in the transmembrane domain or in the ATP binding site [92].

### 2.7 Metal binding domains of ATP7B

The yeast ATP7B homolog Ccc2 has two MBDs, the bacterial counterpart has one MBD and *C.elegans* Cu-ATPase has three metal binding domains [10]. MBDs are the initial entry point of Cu(I) in Cu-ATPases and are primarily responsible for receiving Cu(I) from a chaperone [76]. The six metal binding domains in ATP7A and ATP7B are connected by peptide linkers of various length. The MBDs in ATP7B are numbered starting from the first MBD in the N-terminal region, with MBD6 being the nearest MBD to the membrane-spanning part of ATP7B. The N-terminal MBD's consists of 630 residues that are nearly half the size of the full-length protein. Among 630 residues, 200 residues belong to the inter-domain linkers. The linker that connects MBD4 and MBD5 consists of 76 residues which is the longest among other linkers. The linker between MBD2-MBD4 is 29 residues long, between MBD2-MBD3 is 24 residues in length, between MBD1-MBD2 is 13 residues and 6 residues between MBD5-MBD6 [12, 80]. To date, the exact roles of all six metal binding domains in ATP7B has not completely understood. Previous *in-vitro* studies have suggested domain-domain interactions occur among MBDs. Also interactions between MBDs and the core (transmembrane segment) of ATP7B have been described [93]. The function of the intramolecular interactions *in vivo* is not yet known. The disease-causing mutation in ATP7B can also be seen in MBD's. Localization studies on ATP7B have reported that the Golgi retention signal is present in the N-terminal MBD and deletion of MBDs in ATP7B cause mislocalization [94]. Each MBD of ATP7B has ferredoxin-like fold (Figure 9) and Cu(I) binding motif similar to that of Atox1. The Cu(I) binding site is present in the solvent exposed loop between β1 and α1 helix. All MBDs have similar Cu(I) binding affinity [76].

There is no clear evidence suggesting MBDs interaction with other domains in vivo, but it has been shown that removal of MBDs in ATP7B have effects in phosphorylation and Cu transport activity. However, in vitro studies have shown MBD interaction with N- and A- domains. The MBD was co-purified with the N-domain and the interaction was found to be present in absence of Cu in the MBDs. This interaction was proposed to keep the ATP7B in inactive at low Cu levels [95]. Cu binding to MBD induced structural rearrangement resulting in disruption of MBD and N-domain interaction, and allowing ATP to bind N-domain [96]. Similar to MBD-N-domain interaction studies, the interaction between N-terminal MBDs and the A-domain was observed by co-purification experiment. Copper binding to the N-terminal MBDs was reported to enhance the interaction between MBDs and the A-domain and the interaction was found to stabilize the protein during ER to Golgi cargo [97].

Some studies have revealed that there is strong interaction between MBDs that help to mobilize Cu(I) in ATP7B [93]. A study on anti-ATP7B nanobodies binding to 1-6 MBDs in ATP7B showed that the interaction between MBDs is transient and that these interactions are responsible for the localization of ATP7B [84].

It was hypothesized that Cu binding to MBDs of ATP7B induces conformational changes along the N-terminal region of the protein. However, *in vitro* observation on ATP7B's MBDs has provided evidence that the Cu binding to MBDs causes some localized changes in the Cu binding loop but does not affect the overall N-terminal MBDs [80].

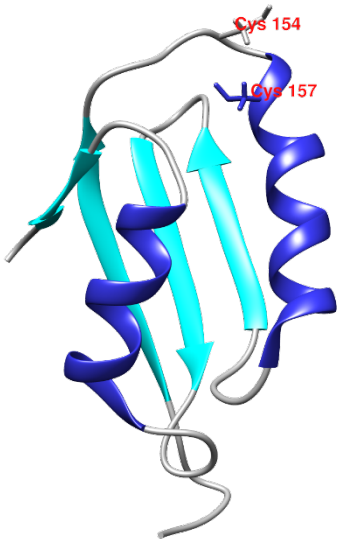


**Figure 9:** Secondary Structure illustration of Metal binding domain 2 of human Cu-ATPase ATP7B. The MBD2 structure is exactly similar to human Cu chaperone Atox1 (Solution structure of MBD2, Pdb: 2LQB). The Cu(I) binding motif are labeled in red (cysteine residues at 154 and 157 site).

### 2.8 The Golgi luminal loop of ATP7B

The copper transport by Cu-ATPases involves hydrolysis of ATP and the formation of phosphorylated intermediates (catalytic cycle). Cu(I) binding to the intramembrane sites initiates the ATP hydrolysis and phosphorylation step. The protein dephosphorylation is activated when the Cu is discharged from the intramembrane sites into lumen. Studies on ATP7A have suggested that the luminal loop segment connecting the transmembrane domain 1 and 2 is important for Cu release. Mutation in the loop does not affect the ATP hydrolysis and phosphorylation but inhibits subsequent dephosphorylation [98]. In both ATP7B and ATP7A, there are four luminal protruding loops and each loop links two transmembrane domains. The luminal loop region that connects TMD1 and TMD2 in ATP7A and ATP7B contains numerous histidine and methionine residues in comparison to other luminal loop segments. Notably, the proposed luminal segment is longer in ATP7A than ATP7B and Cu(I) binding to this region in ATP7A involves His and Met residues [98]. Two distinct Cu(I) binding sites (3-coordinated site (His-$(Met)_2$ site), and 2-coordinate site His-His or His-Met site) have been reported in this luminal loop segment and the segment is displayed as final Cu release site in ATP7A before Cu is loaded to the Cu dependent enzymes via protein-protein interaction or direct binding of Cu[14]. In ATP7B, the luminal loop has many methionine and histidine residues, but slightly less than ATP7A. There is limited knowledge on Cu release in ATP7B.

## 2.9 Yeast Complementation assay

There have been studies of ATP7B mediated Cu transport and localization in various cell types, including HepG2, neuronal cells, and cancerous cells, [36, 90, 94], as well as model systems such as LEC rats, ATP7B deficient mice, and drosophila [99]. ATP7B localization studies are mostly carried out in mammalian cell types [100]. The Cu-ATPase transport activity is most extensively studied in yeast [101], while ATP phosphorylation activity has been primarily observed *in vitro* experiments [11]. The Cu homeostasis pathway is well characterized in yeast *S.cerevisiae* through genetic and biochemical analysis [102]. The proteins involved in the Cu transport are functionally conserved between yeast and mammals. Specifically, the mammalian proteins Ctr1, Atox1, and ATP7A/B are orthologues of the yeast proteins Ctr1, Atx1, and Ccc2 respectively. Due to this functional conservation, yeast can be used as a molecular model to understand mammalian Cu homeostasis at the cellular and molecular level[102].

A functional assay for ATP7B was established based on the complementation of yeast homolog *CCC2*. The assay provides an easy means to study protein function. The ATP7B expressed in yeast mediate wildtype Fet3 activity and wildtype growth rates in iron-limited conditions implicating that human ATP7B functions in yeast and can thus complement the yeast *CCC2* deletion mutant, and restore the wildtype phenotype of growth on media with limited iron [15]. It was found that Cu loaded Fet3, complexes with Ftr1p, for high-affinity iron uptake in yeast. Fet3 acts as a marker for intracellular Cu transport [103]. Numerous studies have been carried out to understand the mutational effects of the human ATP7B in transport function in yeast [101].

This type of assay is an excellent tool to examine the different ATP7B mutations. The assay was widely used to determine the degree to which Wilson's disease mutations affects the function of ATP7B and as a biochemical probe to understand the molecular mechanism of a WD variant and the functional roles of ATP7B in Cu homeostasis[15]. For patients, it is of vital importance to determine how their specific mutation in ATP7B is likely to cause disease and thus help design an early treatment for the WD patient to prevent liver damage. Yeast based complementation techniques has been used for studying the functional role of mammalian transport protein Nramp2 [104] and CFTR [105]. Expression of Nramp2 (yeast homologue Smf2, resistance to EGTA) and CFTR (yeast homologue Ste6, chloride channel) rescue the growth phenotype in ΔSmf2 and ΔSte6 yeast strain. The growth rate of the yeast strain in limiting condition (high concentration of EGTA (ΔSmf2) and less chloride concentration (ΔSte6)) is correlated with the protein activity. The significance of NBD in CFTR protein was studied using yeast complementation assay [105].

# 3. MATERIALS AND METHODS

In this chapter, the experimental methods used in the thesis are described. First, the yeast strains and plasmid constructions are explained, followed by the description of the working principle of yeast complementation assay. Further, the experimental setup of the yeast complementation assay is explained. The background is also provided on NMR spectroscopy and molecular dynamics simulations.

## 3.1 Yeast strain and Plasmid Construction

### Yeast strains

Yeast *Saccharomyces cerevisiae* CEN.PK 113-11C (*MATa SUC2 MAL2-8 URA3-52 HIS3-Δ1*) was used as reference strain (Dr. P. Kötter, Institute of Microbiology, Johann Wolfgang Goethe-University, Frankfurt, Germany). The strain has a mutation in *CYR1* (codes for adenylate-cyclase and generates cAMP) which leads to high-stress resistance during active fermentation and growth. Yeast strains were cultivated on YEPD/YPD (Yeast Extract Peptone Dextrose) media as described previously [106].

### Bacterial strains

*E. coli* was used for plasmid constructions. The *E. coli* DH5α strain was cultivated on Luria-Bertani (LB) broth medium (10 g/L tryptone, 5 g/L yeast extract, 10 g/L NaCl), or on plates with the same composition with the addition of 20 g/L agar. The preparation of competent E. coli cells and transformations were carried out according to standard protocols[107]. Ampicillin was added when required (80 µg/ml).

### Construction of CCC2 and Atx1 yeast deletion strains

The yeast homologs of human *ATP7B* and *ATOX1* genes, *CCC2* and *ATX1*, are located on chromosomes IV and XIV of *S. cerevisiae*, respectively. The *Δccc2*, *Δatx1* and *Δccc2Δatx1 S. cerevisiae* strains were constructed by deletion of *CCC2* and *ATX1* genes individually, and in combination. Deletions of *CCC2* and *ATX1* genes were performed by replacing the gene with a KanMX deletion cassette which carries the kanamycin selectable marker. The double-deletion strain was constructed by first replacing the *CCC2* gene with a KanMX deletion cassette followed by disruption of the kanamycin marker and then replacing the other (*ATX1*) gene with the KanMX cassette. The KanMX deletion cassette consists of loxP sites flanking both ends of the kanamycin marker [108]. Disruption of kanamycin was introduced by transforming with a

Crelox plasmid pSH47 (Ura- marker, Cre gene, GAL1 promoter) [109] which integrates at the loxP sites on both ends of the marker via the expressed Cre recombinase when grown in galactose medium. Elimination of the kanamycin marker was confirmed, followed by removal of cells containing the pSH47 plasmid by plating on 5-fluoroorotic acid. All deletion strains and modifications were constructed by standard PCR techniques and homologous recombination.

**Plasmid constructions**

The human *ATP7B* and *ATOX1* genes were cloned in separate plasmids. The plasmids p426GPD (ATCC 87361; GPD, promoter for expression; Ura3 and ampR, markers) and p423GPD (ATCC 87355; GPD, promoter for expression; His3 and ampR, markers) were used as vector plasmids for *ATP7B* and *ATOX1* genes, respectively. The *ATP7B* sequence was recloned from a plasmid from Dr. A Koc [101], whereas the *ATOX1* gene was obtained from a plasmid designed in our lab [67]. The *ATP7B* (including constructs with deleted MBDs or mutated variants) and *ATOX1* genes were amplified with BamHI and SalI restriction sites. Created ATP7B modified constructs were as follows: domain deletions of one MBD to all six MBDs in the *ATP7B* gene (i.e., ATP7B 1DEL, ATP7B 1-2DEL, ATP7B 1-3DEL, ATP7B 1-4DEL, ATP7B 1-5DEL, and ATP7B 1-6DEL) and point-mutations in the *ATP7B* gene (i.e., ATP7B CPC-to-SPS, with two Cys replaced with Ser in transmembrane domain 6, and D1027A, with the transiently phosphorylated Asp1027 replaced by Ala) (Figure 10B). The ATP7B luminal loop mutants with all of M668, M671, H679, M682, and H686 mutated to Ala, or only all His mutated to Ala, or only all Met mutated to Ala, or the single mutation M682A were constructed. Mutations were introduced into the full length ATP7B by Quick-change site directed mutagenesis kit using the constructed p426GPD-ATP7B plasmid [110] as a template. All constructed plasmids were verified by sequencing (Eurofins). Plasmids were chemically transformed into yeast cells by the standard lithium-acetate method [111] and grown on selective media: SD-Ura- for the p426GPD vector, SD-His- for the p423GPD vector and SD-Ura-His- for yeast with both plasmids. Constructed plasmids are listed in Table 1.

**Table 1:** List of constructed plasmids

| No | Plasmid | Genotype and description | Paper |
|---|---|---|---|
| 1 | ATOX1 wildtype | Human ATOX1 (191 bp) gene cloned into p423GPD vector (GPD promoter, CYC1 terminator, and ampR,HIS3 selection marker) | I,II |
| 2 | ATP7B wildtype | Human ATP7B gene (4398 bp) cloned into p426GPD vector (GPD promoter, CYC1 terminator, and ampR,URA3 selection marker) | I,II |
| 3 | ATP7B 1DEL | Human ATP7B gene (375 – 4398) cloned into p426GPD vector (GPD promoter, CYC1 terminator, and ampR,URA3 selection marker) | I |
| 4 | ATP7B 1-2DEL | Human ATP7B gene (630 – 4398) cloned into p426GPD vector (GPD promoter, CYC1 terminator, and ampR,URA3 selection marker) | I |
| 5 | ATP7B 1-3DEL | Human ATP7B gene (981 – 4398) cloned into p426GPD vector (GPD promoter, CYC1 terminator, and ampR,URA3 selection marker) | I |
| 6 | ATP7B 1-4DEL | Human ATP7B gene (1278 – 4398) cloned into p426GPD vector (GPD promoter, CYC1 terminator, and ampR,URA3 selection marker) | I |

| | | | |
|---|---|---|---|
| 7 | ATP7B 1-5DEL | Human ATP7B gene (1665 – 4398) cloned into p426GPD vector (GPD promoter, CYC1 terminator, and ampR,URA3 selection marker) | I |
| 8 | ATP7B 1-6DEL | Human ATP7B gene (1893 – 4398) cloned into p426GPD vector (GPD promoter, CYC1 terminator, and ampR,URA3 selection marker) | I |
| 9 | ATP7B CPC-to-SPS | Human ATP7B gene (mutation of CPC motif (TGC…TGC) to SPS motif (TCC…TCC) (at gene position 2947-2949 and 2953-2955)) cloned into p426GPD vector (GPD promoter, CYC1 terminator, and ampR,URA3 selection marker) | I |
| 10 | ATP7B D1027A | Human ATP7B gene (mutation of aspartic acid (GAC) to alanine (GCC) (at gene position 3079-3081)) cloned into p426GPD vector (GPD promoter, CYC1 terminator, and ampR,URA3 selection marker) | I |
| 11 | ATP7B M682A | Human ATP7B gene (mutation of methionine (ATG) to alanine (GCG) (at gene position 2044-2046)) cloned into p426GPD vector (GPD promoter, CYC1 terminator, and ampR,URA3 selection marker) | II |
| 12 | ATP7B M3A (mutation of M668, M671 & M682 residue to alanine) | Human ATP7B gene (mutation of methionine (ATG) at 668, 671 and 682 sites to alanine (GCG) (at gene position 2002-2004,2011-2013 and 2044-2046)) cloned into p426GPD vector (GPD promoter, CYC1 terminator, and ampR,URA3 selection marker) | II |
| 13 | ATP7B H2A (mutation of H679 & H684 residue to alanine) | Human ATP7B gene (mutation of histidine (CAC) at 679 and 684 sites to alanine (GCC) (at gene position 2035-2037 and 2050-2052)) cloned into p426GPD vector (GPD promoter, CYC1 terminator, and ampR,URA3 selection marker) | II |
| 14 | ATP7B M3H2A (all five mutations) | Human ATP7B gene (mutation of methionine (ATG) at 668, 671 and 682 sites to alanine (GCG) (at gene position 2002-2004,2011-2013 and 2044-2046) and histidine (CAC) at 679 and 684 to alanine (GCC) (at gene position 2035-2037 and 2050-2052)) cloned into p426GPD vector (GPD promoter, CYC1 terminator, and ampR,URA3 selection marker) | II |

### 3.2 Yeast complementation assay

The copper transport pathway and iron transport pathway are interlinked in all eukaryotes. In yeast, the intracellular copper transport is responsible for the iron uptake and it is well coupled to each other. Fet3 is a multi-copper oxidase (like human ceruloplasmin, type 1 membrane protein with structure consisting of three cupredoxin-like fold) enzyme localized in the plasma membrane also traffics to vesicular compartments. The yeast cytosolic Cu chaperone Atx1 delivers Cu to Ccc2 localized in the Golgi, a Cu-binding ATPase that incorporates Cu into Fet3. The main function of Fet3 is to catalyze the oxidation of $Fe^{2+}$ to $Fe^{3+}$ (ferroxidase reaction, $4Fe^{2+}+4Cu^{2+}\leftrightarrow 4Fe^{3+}+4Cu^{1+}$, $4Cu^{1+}+O_2+4H^+ \leftrightarrow 4Cu^{2+}+2H_2O$) using

oxygen as a substrate. Binding of Cu to Fet3 initiates the oxidase activity, as no oxidase activity is present in apo-Fet3 and Cu bound Fet3 complexes with iron permease Ftr1 which mediates high-affinity iron uptake. The oxidase function of Fet3 is required at the plasma membrane for iron uptake and the $Fe^{3+}$ generated by Fet3 is a ligand for the iron permease Ftr1 which uptake extracellular iron [33]. Taken all together, Ccc2 protein connects the Cu uptake pathway to iron uptake pathway in yeast and therefore, high-affinity iron uptake pathway of yeast cells is strictly dependent on Cu transport[112].

Deletion of yeast copper transport proteins perturb the Cu transport. Disrupted intracellular Cu transport renders yeast deficient in high-affinity iron uptake due to inability to load Cu to Fet3. The yeast grown in iron-limited medium require completely functional copper transport for its survival. Any perturbation in Cu transport results in inactivation of Fet3 enzyme thereby ceased iron uptake in yeast which eventually leads to yeast growth limitations. The Δ*ccc2* yeast model (iron uptake deficient) was initially used to test whether mammalian Cu-ATPase can complement the function of Ccc2. The complementation function of the protein is assessed via growth (growth rate) in iron-limited conditions [15]. The growth rate of the Δ*ccc2* yeast strains in iron-limited conditions is associated with the protein function of Cu-ATPase. The growth rate of the Δ*ccc2* yeast strains was measured during the exponential growth phase since the exponential phase is considered to be the period of balanced uniform multiplication of cells (also nutrients consumption and metabolic activities are known to be higher during exponential phase which involves the highest protein function)[113].

In our work, we used Δ*ccc2*Δ*atx1* yeast strain for investigating the functional role of MBDs and specific residues in the human Cu-ATPase, ATP7B. The Δ*ccc2*Δ*atx1* yeast strain was created by sequential deletions of Cu transporter genes *CCC2* and *ATX1* that are located in the chromosome IV and XIV, respectively. The gene deletions were confirmed by plating the yeast strain in kanamycin selective media. Next, the genes for human Cu transport proteins: *ATP7B* and *ATOX1* were amplified from pAG426GPD-ATP7B and pET-21b-ATOX1, followed by integration of *ATP7B* and *ATOX1* gene into p426GPD and p423GPD high copy plasmid correspondingly. For the constitutive expression of ATP7B (or ATP7B variants) and Atox1 proteins, yeast strains were transformed with p426GPD-ATP7B (or ATP7B variants) and p423GPD-ATOX1 (Figure 10A). All constructed yeast strains were subjected to yeast complementation assay. The growth rate of the yeast strains in iron-limited conditions was calculated. Measuring yeast growth rates in iron-limited medium is a sensitive method that can detect functional differences between mutant ATP7B variants. Numerous studies have been carried out to understand the mutational effect of ATP7B in Cu transport function[101].

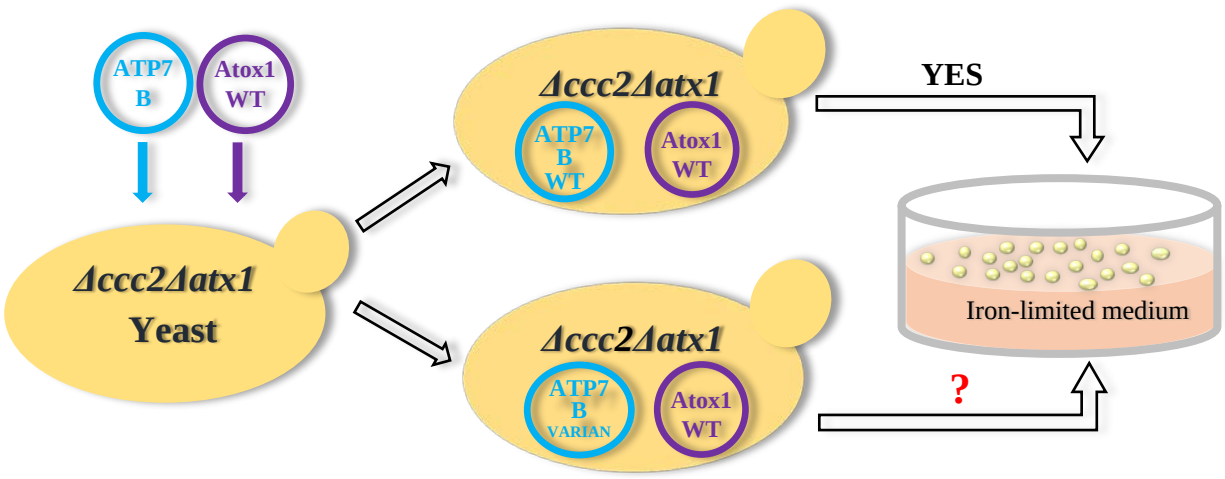

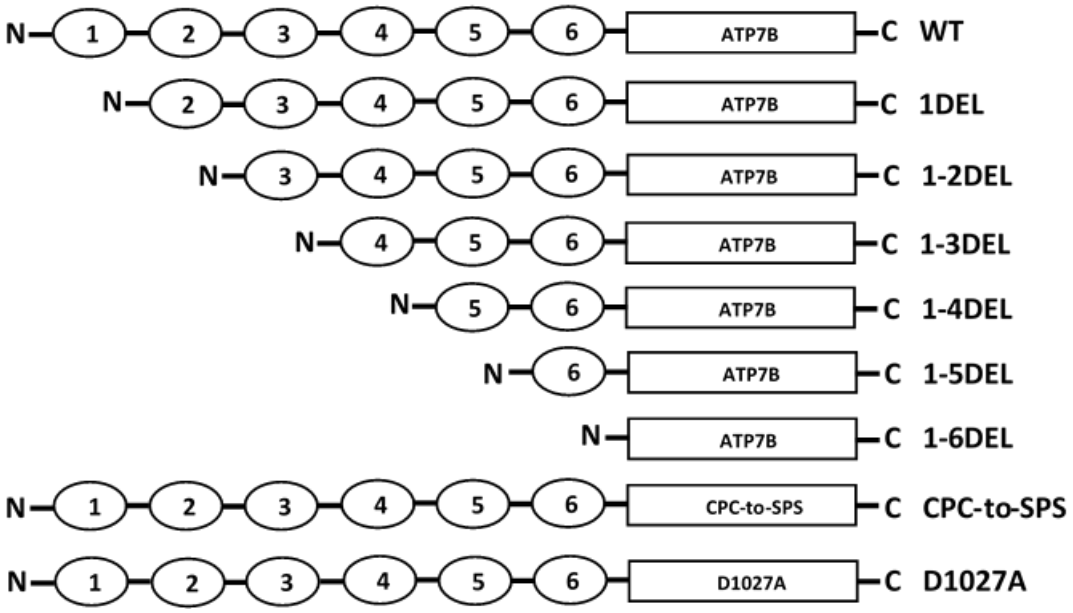


**Figure 10:** Yeast complementation system (**A**) Schematic representation of the double deletion yeast system designed for human Cu transport studies. Plasmids with human *ATP7B* and *ATOX1* were used to complement the yeast strains in which yeast endogenous *CCC2* and *ATX1* genes were deleted individually or in combination. In this system, we have investigated the consequences of wild type, mutated and truncated ATP7B variants by probing cell growth on Fe-limited media which requires functional Cu transport. (**B**) Overview of mutations and MBD deletion constructs of ATP7B that were introduced in the engineered yeast strains.

**Experimental setup**

A synthetic defined (SD) medium containing 1.7 g/L yeast nitrogen base lacking Fe and Cu ions, 50 mM MES buffer pH 6.1, 20 g/L glucose, 5 g/L ammonium sulfate was used in combination with a complete supplement mixture (CSM) (combination of amino acids, vitamins and other essential components to support vigorous growth of yeast cells) with dropout as follows. CSM with -Ura and -His dropout was used for the strain carrying both ATP7B and Atox1 plasmids, whereas CSM with -Ura dropout was used for the strain with the ATP7B plasmid and CSM with -His dropout was used for the strain with the Atox1 plasmid. The Fe-limited medium was prepared from the SD medium with the addition of 1 mM ferrozine (Fe chelator), 1 µM $CuSO_4$ and 100 µM $FeSO_4$. Fe-supplemented medium was prepared without ferrozine and 350 µM $FeSO_4$ and 500 µM $CuSO_4$. For the plating assay, transformants were grown in SD medium with 20 g/L agar. Yeast cells from pre-grown overnight cultures (30 °C, 200 rpm) were diluted to an optical density at 600 nm of 0.1, and then serial dilutions with sterile water were performed followed by plating in Fe-limited and Fe-supplemented medium and incubation at 30 °C for 3 days. All experiments were carried out in identical conditions [10].

**Yeast growth analysis**

ATP7B Cu transport activity of the various yeast strains was evaluated using growth curve analysis in iron-limited medium. A single yeast colony from the plates was inoculated in iron limited medium (SD medium containing 1.7 g/L yeast nitrogen base without Fe and Cu, 50 mM MES buffer pH 6.1, 20 g/L

glucose, 5 g/L ammonium sulfate, complete supplement mixture CSM –Ura –His, 1 mM ferrozine (Fe chelator), 1 µM $CuSO_4$ and 100 µM $FeSO_4$) and incubated over night at 30°C and 200 rpm [10]. Yeast cells from this culture were washed with ice cold deionized water and cultivated in fresh iron limited medium at an initial cell density of $OD_{600}$ = 0.1. The growth of the cells was monitored spectroscopically ($OD_{600}$) for 30 hrs. All yeast growth experiments were carried out at identical conditions. Growth rates were calculated from the linear exponential growth phase ($\Delta\ln(OD_{600})/hr$)[10].

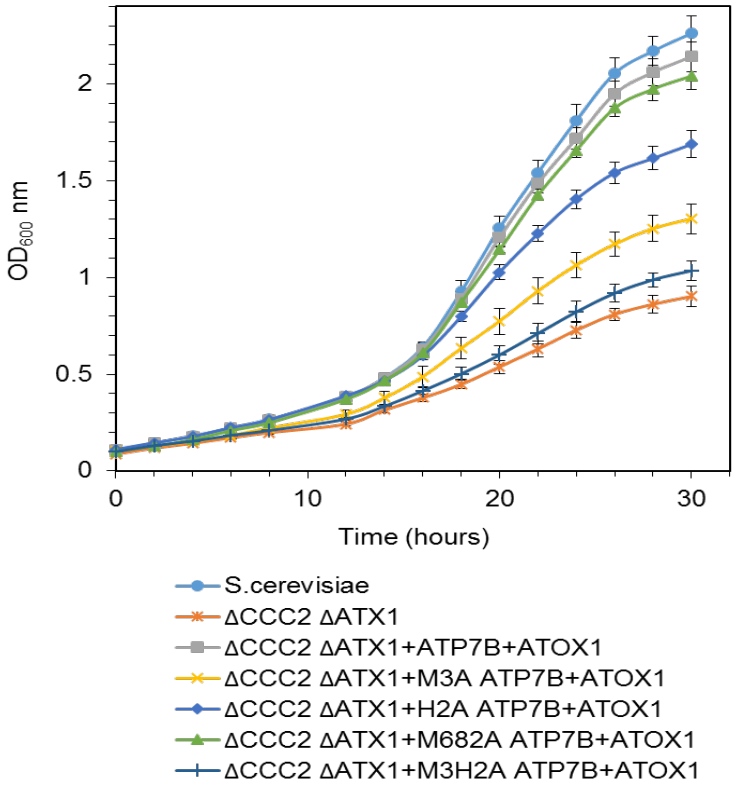


**Figure 11:** Yeast growth Curve. Examples of yeast growth curves, $OD_{600nm}$ versus time, for various combinations of yeast strains and supplementation of high-copy plasmids with human Atox1 and/or ATP7B, as indicated, in iron-limited media.

### 3.3 Protein Extraction and Western Blotting

All yeast strains were grown in iron limited medium for 24 hours at 30 °C. Cell pellets were collected by centrifugation at 2000xg at 4 °C for 10 min, washed twice with ice-cold water and lysed with glass beads (lysis buffer: 50 mM HEPES pH 7.5, 150 mM NaCl, 2.5 mM EDTA, 1% v/v Triton X100 and freshly added protease inhibitor). After lysis, membranes were collected by centrifugation at 18000xg (4 °C, 30 min). Samples were re-suspended in SDS loading buffer (0.5 M Tris-HCl, pH 6.8, 10% SDS, 0.5% (w/v) Bromophenol blue, 87% glycerol, 100 mM DTT) and 50 µg of membranes were loaded on a 4-12 % Bis-Tris gel (Invitrogen) and blotted onto PVDF membranes. ATP7B and Atox1 proteins were detected with monoclonal rabbit ATP7B and Atox1 antibodies, respectively (Abcam, 1:1000 dilution), upon incubation overnight, 4°C. Next, blots were incubated with horseradish peroxidase conjugated anti-rabbit IgG reagent (Thermo Scientific Pierce) for 15 min, 4°C. Bands were detected by Pierce™ Fast Western Blot Kits,

SuperSignal™ West Femto, Rabbit (Thermo Scientific Pierce) and visualized with a BioRad ChemiDoc XRS image analyzer.

### 3.4 Cellular Localization of ATP7B

Yeast cells were cultured to mid log phase in iron-limited medium. Harvested yeast cells were fixed in 5 ml of 50 mM $KPO_4$ (pH 6.5), 1 mM $MgCl_2$ and 4 % formaldehyde for 2 h. After fixation, the cells were washed two times in 5 ml of PM buffer (100 mM $KPO_4$ pH 7.5, 1 mM $MgCl_2$) and followed by resuspension in PMST buffer (100 mM $KPO_4$ pH 7.5, 1 mM $MgCl_2$, 1 M sorbitol, 0.1 % Triton X-100) to a final $OD_{600}$ of 10. 100 µl yeast cells were incubated for 20 min in 0.6 µl of β-mercaptoethanol and 1 mg/ml zymolyase (Zymo Research). The spheroplasted cells were washed with PMST buffer and attached to polylysine-coated coverslips. Adherent cells were blocked in PMST-BSA buffer (0.5 % BSA in PMST buffer) for 30 min. Next, the adherent cells were incubated overnight at 4 ◦C with primary antibody (1:500 rabbit monoclonal ATP7B antibody, Abcam) diluted in PMST-BSA buffer. After incubation, the cells were washed three times with PMST-BSA buffer and incubated with secondary antibody (1:1000 anti-rabbit Alexa 488, Abcam) for 3 h at room temperature, and with 0.4 mg/ml DAPI (staining nuclei) for 5 min. Cells were mounted in Vectashield mounting medium (Vector Laboratories). Images were acquired using a Leica DM 2000 inverted microscope and processed with the Leica application suite (LAS-AF lite) software.

## 4. SUMMARY OF RESULTS

This chapter presents an overview of results from my two studies. All the results summarized here are the compilation of experimental work from the paper I and II. For more details about the presented research, the reader is referred to the appended papers.

### 4.1 Expression of human ATP7B and ATOX1 in humanized yeast system

The Δ*ccc2*Δ*atx1* yeast was supplemented with *ATP7B* and *ATOX1* gene on high copy plasmids for the constitutive expression of human ATP7B and Atox1 proteins. The expression of ATP7B and Atox1 proteins in yeast were confirmed by western blotting and the molecular weight of the ATP7B (163 kda) and Atox1 (7.5 kda) bands agrees well with the predicted molecular weight (Figure 12 A). Expression amount of the ATP7B mutants were similar to the ATP7B wildtype. Like ATP7B expression, the human Atox1 protein showed efficient expression in Δ*ccc2*Δ*atx1* yeast (Figure 12B). The expression amounts of domain-deleted ATP7B variants were similar to ATP7B wildtype. As expected, the domain-deleted ATP7B variants had reduced molecular size compared to ATP7B. The molecular weight of domain-deleted ATP7B variants obtained from the western blotting analysis are as follow: ATP7B 1DEL (150 KDa), 1-2DEL (140 KDa), 1-3 DEL (125 KDa), 1-4DEL (115 KDa), 1-5DEL (100 KDa), and 1-6DEL (90 KDa).

**A**

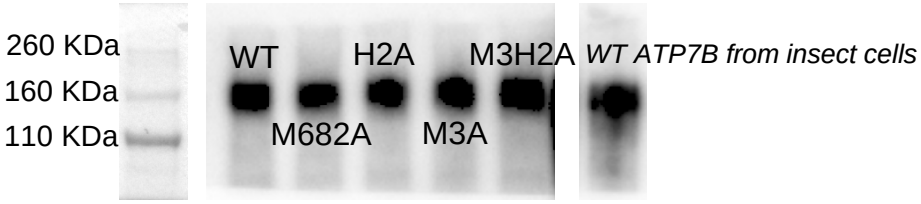

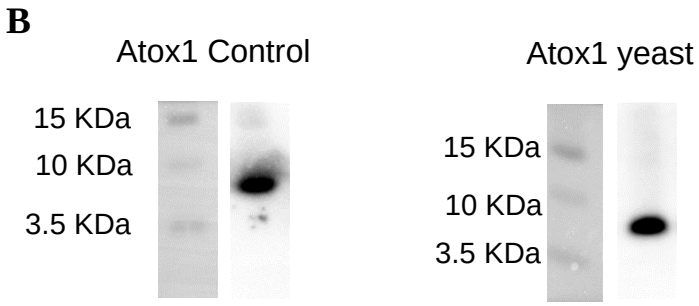


**Figure 12:** Expression of ATP7B and Atox1. Western blot analysis of Atox1 and ATP7B expressed in Δ*ccc2*Δ*atx1* yeast strain using specific ATPB and Atox1 antibody**.** (**A**) Expression of human Cu ATPase ATP7B in yeast (Left to right 1. Wild-type ATP7B; 2. M682A in ATP7B; 3. H2A in ATP7B, 4. M3A in ATP7B; 5. M3H2A in ATP7B; 6. Wild-type ATP7B expressed in insects cells as control.) (**B**) Expression of human Cu chaperone Atox1 in yeast (Left: purified Atox1 as control, Right: Atox1 expressed in yeast)

### 4.2 Yeast complementation assay

The constructed yeast strains *(*Δ*ccc2*, Δ*atx1* and Δ*ccc2*Δ*atx1*) are high-affinity iron uptake deficient due to the lack of Cu delivery to Fet3. Under iron limited conditions, the high-affinity iron uptake is vital for yeast survival. Therefore, these strains were unable to thrive on iron limited medium because of the absence of functional Fet3 (high-affinity iron uptake deficient) (Figure 13). The growth of these strains was rescued in the presence of high iron or high Cu concentrations. The reason for the growth in high iron conditions (iron supplemented medium) might be due to the fact that iron enters the yeast cell via low-affinity iron uptake pathways or Cu binds to the apo-Fet3 when localized at the cell surface. Expression of human ATP7B protein in Δ*ccc2* background and human chaperone Atox1 in Δ*atx1* strains rescued the viability in an iron limited medium. Earlier studies have reported that ATP7B expression in Δ*ccc2* yeast and Atox1 expression in Δ*atx1* yeast complements the function of Ccc2 and Atx1. The viability of the Δ*ccc2*Δ*atx1* yeast was not restored by the expression of either ATP7B or Atox1 protein whereas complementation of both proteins enabled the yeast viability under iron limited conditions (Figure 13).

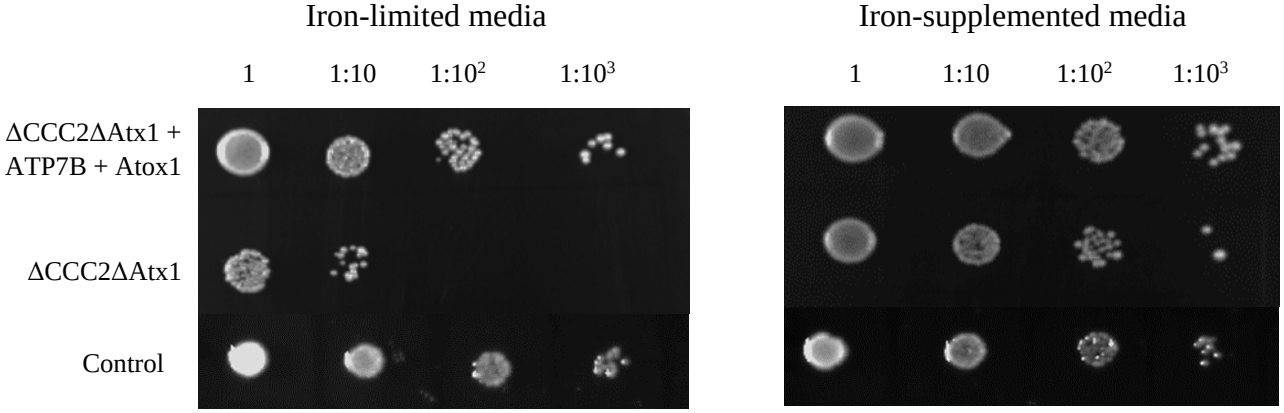

**Figure 13:** Yeast complementation assay. Plating assay showing serial decimal dilutions of Δ*ccc2*Δ*atx1* yeast cells, without and with added Atox1 and ATP7B plasmids, as well as control (wild-type) yeast, spotted onto a agar plate prepared with Fe-limited and Fe-supplemented media.

Exponential growth rate of the yeast in iron-limited conditions relates to the Cu transport efficiency. The exponential growth rates of the yeast strains grown in iron limited conditions was determined. As expected the Δ*ccc2*, Δ*atx1* and Δ*ccc2*Δ*atx1* strains had a poor growth rates in iron-limited conditions. However, the growth of Δ*ccc2* and Δ*atx1* yeast were restored when complemented with corresponding human Cu transport proteins ATP7B and Atox1. The growth data revealed that the deletion of one yeast genes and complementing it with a corresponding human gene restored the wildtype phenotype. Like in the plating assay, Δ*ccc2*Δ*atx1* yeast growth was recovered by expression of both ATP7B and Atox1 proteins and growth was restored similar to reference strain in iron-limited conditions (Figure 14). This suggests that both ATP7B and Atox1 are pivotal for the Cu transport in yeast in the absence of yeast Cu transport proteins Ccc2 and Atx1.

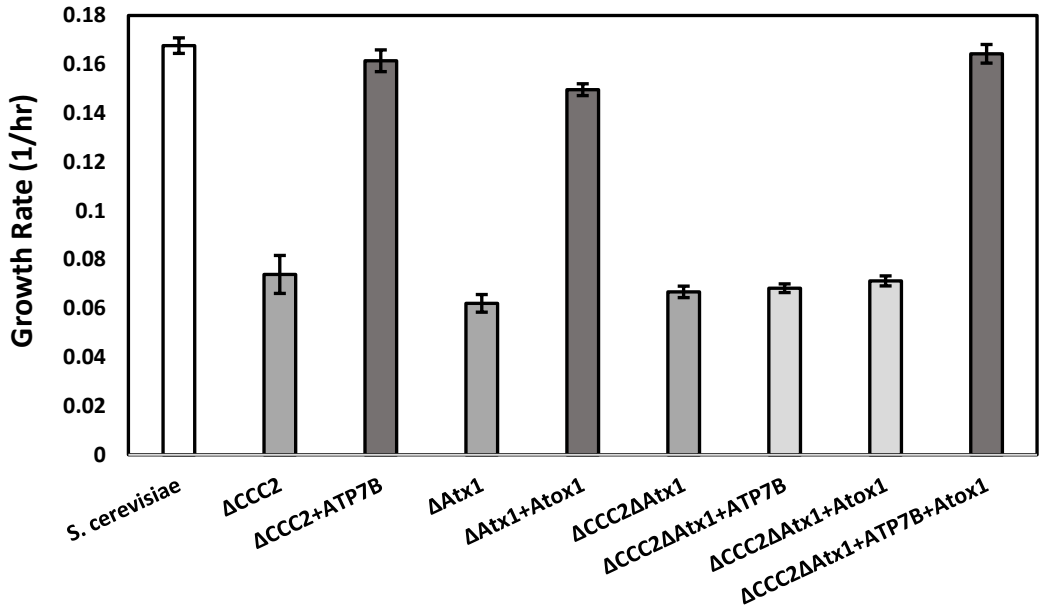


**Figure 14:** Growth rates for *Δccc2*, *Δatx1*, *Δccc2Δatx1* yeast strains complemented with ATP7B and Atox1 plasmids, under Fe-limited conditions. Error bars are based on the standard deviation for duplicate experiments.

The results here show that, ATP7B and Atox1 proteins can effectively complements the function of Ccc2 and Atx1 proteins. However, ATP7B expression alone did not recover the growth in Δ*ccc2*Δ*atx1* which implies that Atox1 (or Atx1) is essential for Cu transport. Employing Δ*ccc2*Δ*atx1* yeast model in complementation assay enable us to study the role of human Cu-ATPases and human Cu chaperones in Cu transport. Previous studies have used Δ*ccc2* yeast model in the complementation assay for functional analysis of ATP7B and in that the model system utilize yeast Cu chaperone Atx1 to shuttle Cu to ATP7B. The yeast model we established here *(*Δ*ccc2*Δ*atx1*) can mimic the real human cellular Cu transport. Thus, the designed system was used in this research work to unravel the roles of six MBDs (Paper I) and luminal loop (Paper II) of ATP7B.

### 4.3 Metal binding domains in ATP7B mediated Cu transport

Different domain truncated ATP7B variants were constructed in order to assess the role of MBDs of ATP7B in Cu transport. Truncated ATP7B variants are created in which all N-terminal MBDs are deleted in succession (Figure 10B). Apart from this, CPC to SPS ATP7B and D1027A ATP7B variants were also constructed in this work. The CPC motif lies inside the ion transduction domain of ATP7B and D1027A mutation in the phosphorylation domain. Previous studies have shown both these ATP7B variants completely block Cu transport [114], hence these variants are used here as a negative control.

The growth rates of the Δ*ccc2*Δ*atx1* yeast strain with different ATP7B variants and in presence of wildtype Atox1 were determined. Western blot analysis confirmed that the expression amounts of ATP7B variants were very similar to that of wildtype ATP7B. The molecular size of truncated ATP7B variants matches the theoretical molecular size for ATP7B protein. The growth rates for CPC to SPS and D1027A mutations were similar to the growth rate of yeast strain lacking ATP7B and Atox1 expression. Moreover, deleting the first N-terminal metal binding domain of ATP7B (ATP7B 1DEL) decreased the growth rate to 70% which indicates that the MBD1 is important for making Cu transport efficient. Removal of first and second metal binding domain (ATP7B 1-2DEL) had also similar growth rate to that of ATP7B 1DEL (Table 2). However, removal of third MBD (ATP7B 1-3DEL) restored the growth behavior like wildtype ATP7B which can be interpreted as ATP7B mediated Cu-transport is restricted by MBD3. Removal of MBD 1-4 (ATP7B 1-4DEL) and MBD 1-5 (ATP7B 1-5DEL) had similar growth like wildtype ATP7B. However, deletion of all six metal binding domains (ATP7B 1-6DEL) in ATP7B resulted in a drastic reduction of growth rate, similar to that of negative controls (Figure 15) which means that the Cu-transport is diminished when the N-terminal MBDs are removed. This result suggests that some of the metal binding domains are pivotal for ATP7B activity and further, indicates that Atox1 delivers Cu to one of the six metal binding domains of ATP7B.

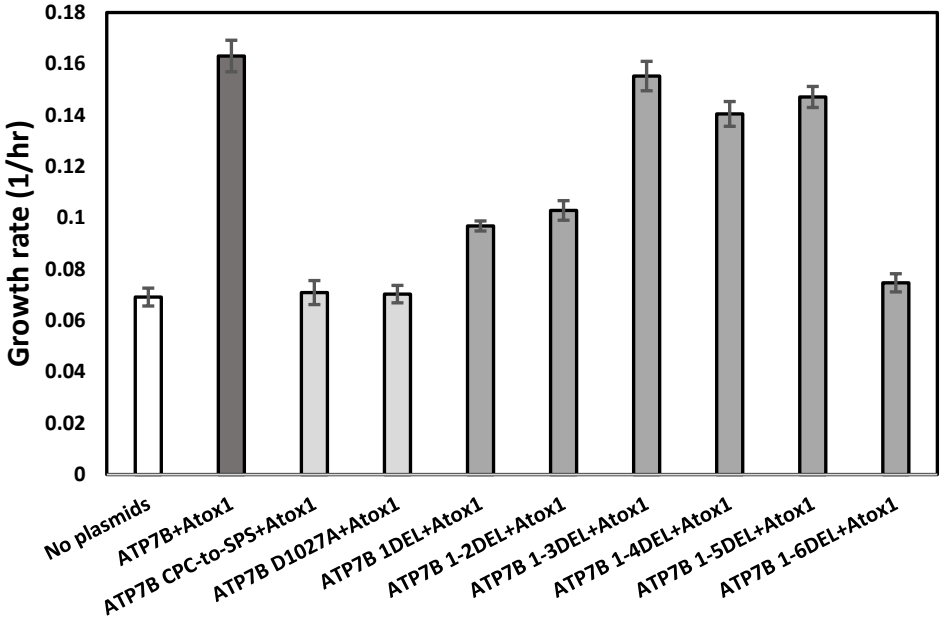


**Figure 15:** Growth rate of domain-deleted ATP7B. Growth rates of the *Δccc2Δatx1* yeast strain complemented with wild type human Atox1 plasmid and the various human ATP7B variants under Fe-

limited conditions as indicated. Error bars are based on standard deviations calculated for duplicate experiments.

Taken all together, it can be concluded that the presence of MBD1 promotes ATP7B mediated Cu transport whereas MBD3 presence limits Cu transport such that these negative effects might be cancelled out by interdomain interactions (MBD1-MBD3 interactions) in full-length ATP7B. As ATP7B 1-3DEL, ATP7B 1-4DEL and ATP7B 1-5DEL had similar growth, it appears that MBD 4 and 5 do not regulate ATP7B mediated Cu transport individually. Previous studies have demonstrated that the ATP7B mediated Cu transport was functional in absence of Cu binding sites in MBD6 [100]. This signifies that the presence of sixth metal binding domain is not sufficient enough for ATP7B mediated Cu transport.

The yeast with CPC to SPS and D1027A mutations had similar growth to yeast which lack ATP7B and Atox1 complementing protein expression. Previous work on these mutants in Δ*ccc2* yeast has reported nonfunctional Cu transport which agrees with our results. The Cu transport of these variants showed non-operative behavior also in the presence of Atox1. The CPC motif and aspartic acid residue (D) in the phosphorylation domain are both essential for ATP7B mediated Cu transport

**Table 2.** Relative growth rates of ATP7B variants in the *Δccc2Δatx1* yeast strain (Figures 14 and 15). The growth rate of the deletion strain alone (*Δccc2Δatx1*) is set to 0 % and the growth of the yeast strain complemented with both wild type plasmids (*Δccc2Δatx1 + ATP7B + ATOX1*) is set to 100 %. Only wild type Atox1 was used here.

| ATP7B variant | ATOX1 | MBD Presence | Relative growth rate (%) |
|---|---|---|---|
| No | no | none | 0 % |
| Wild type | no | MBDs 1-6 | 4 % |
| No | yes | none | 6 % |
| Wild type | yes | MBDs 1-6 | 100 % |
| ATP7B 1-6DEL | yes | no MBDs | 6 % |
| ATP7B 1-5DEL | yes | MBD 6 | 83 % |
| ATP7B 1-4DEL | yes | MBDs 5 and 6 | 76 % |
| ATP7B 1-3DEL | yes | MBDs 4-6 | 92 % |
| ATP7B 1-2DEL | yes | MBDs 3-6 | 35 % |
| ATP7B 1DEL | yes | MBDs 2-6 | 30 % |
| ATP7B CPC-to-SPS | yes | MBDs 1-6 | 2 % |
| ATP7B D1027A | yes | MBDs 1-6 | 1 % |

### 4.4 Role of Atox1 vs Atx1 in yeast Cu transport

The ATP7B domain truncated variants were tested in the absence of Atox1 in Δ*ccc2*Δ*atx1* yeast. It is observed that the growth rates of all truncated variants and wildtype ATP7B corresponded to that of negative controls. This confirms that Cu chaperone Atox1 is essential for the delivery of Cu to ATP7B.

To check whether the yeast Cu chaperone Atx1 can fulfill the role of human Cu chaperone Atox1, the truncated ATP7B variants were expressed in the Δ*ccc2* background, and grown in iron-limited condition. The growth rates of these strains were similar to those strains where the same ATP7B variants were expressed in Δ*ccc2*Δ*atx1* background (Figure 16). This confirms that the Atx1 protein is involved in Cu delivery to Cu-ATPase ATP7B in yeast. Interestingly, this result also indicates that the yeast Cu chaperone Atx1 is as efficient in Cu delivery as human Atox1.

Similar growth profiles observed for truncated ATP7B variants in Δ*ccc2* and Δ*ccc2*Δ*atx1*(+*ATOX1*) backgrounds indicates that ATP7B domain-deleted variants affect internal Cu-transport process but not Cu receiving from chaperone. Cu and ATP binding to ATP7B is most likely involved in the regulation of intra and inter-domain interactions of MBDs and ATP binding domain. This collective feature of ATP7B (both binding and intra/inter-domain interactions) contributes to the overall activity of wildtype ATP7B. The reason for the decreased growth observed in the truncated ATP7B variants is likely due to the perturbation in one or more of the internal domain interactions. To obtain a clear picture about the overall ATP7B activity, ATP hydrolysis and Cu transport kinetic parameters of purified ATP7B variants are required.

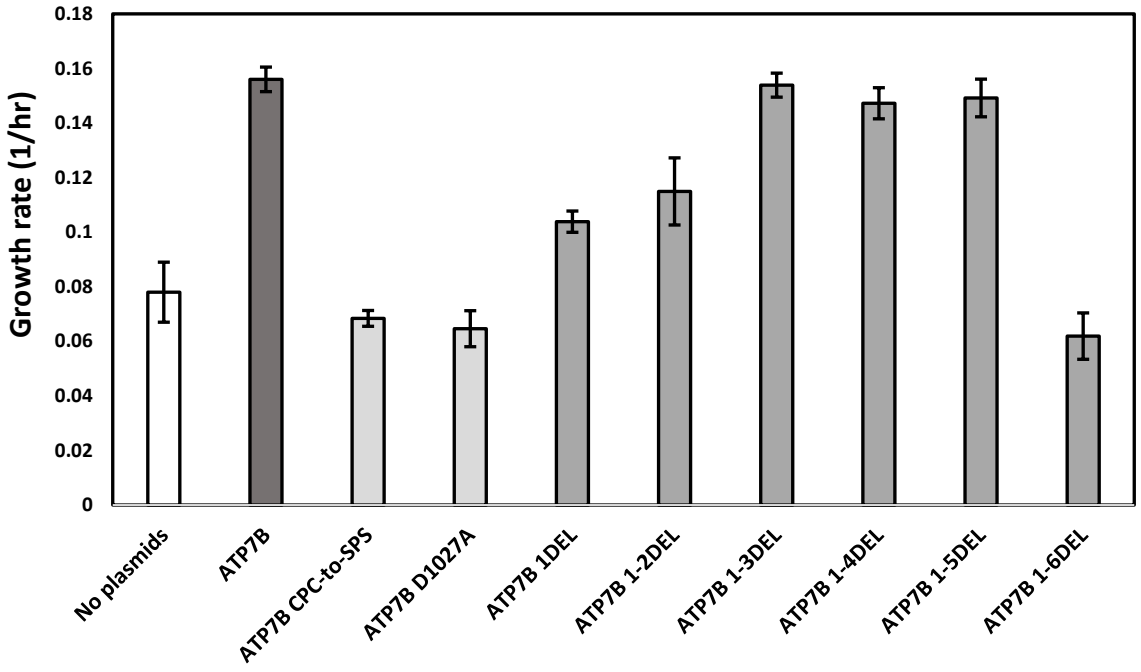


**Figure 16:** Domain-deleted ATP7B variant in *Δccc2* yeast. Growth rates of various ATP7B variants expressed on plasmids in *Δccc2* background yeast strain (in exponential phase) in the absence of the Atox1 plasmid (but here with endogenous Atx1 gene intact) in Fe-limited media. Error bars are based on the standard deviations of duplicate measurements. Note that trends here for various MBD deletions follow the same trends as those in Figure 4 (with human Atox1 instead of Atx1)

In summary, Paper I demonstrates that the developed yeast model system is a valuable tool to study the role of MBDs in ATP7B mediated Cu transport. Presence of at least one N-terminal MBD is required in ATP7B to receive Cu from human Cu chaperone Atox1.

### 4.5 Role of the luminal loop in ATP7B

To understand the functional role of the luminal loop (Paper II) that connects transmembrane domain 1 and 2 in ATP7B, four different ATP7B variants were constructed in which all putative Cu binding residues in the luminal segment (histidine and methionine residues) are mutated into alanine (A). The proposed luminal loop contains three methionine (668, 671 and 682 site in full length ATP7B or M2, M5 and M16 site in the peptide) and two histidine residues (679 and 686 site in full length ATP7B or H13 and H20 site in the peptide) which are anticipated to be Cu(I) binding sites (Figure 17). The constructed ATP7B variants are denoted as i) H2A (mutation of both histidine residues in luminal loop to alanine), ii) M3A (mutation of all methionine residues in luminal loop to alanine), iii) M682A (Mutation of methionine residue at 682 site to alanine) and iv) M3H2A (mutation of all histidine and methionine residues in luminal loop).

| | | | |
|---|---|---|---|
| *Human* **ATP7B** | 654 | FLCSLVFGIPVMALMIYMLIPS----------NEPHQSMVLDHNIIPGLSILNLIFFILCTFVQ | 707 |
| *Human* **ATP7A** | 654 | FLVSLFFCIPVMGLMIYMMVMDHHFATLHHNQNMSKEEMINLHSSMFLERQILPGLSVMNLLSFLLCVPVQ | 724 |
| *L.pneumophila* **CopA** | 85 | FWIALMLTIPVVILE--MGG----------HGLKH----FISG-NGSSWIQLLLATPVV | 126 |
| *S.cerevisiae* **Ccc2** | 262 | ----TLLAIICMLL--YMIVPMM-WPTIVQ----------DRIFPYKETSFVRGLFYRDILGVILASYIQ | 326 |

**Figure 17:** Alignment of luminal loop and nearby transmembrane sequences. Met and His residues are indicated with bold letters and the peptide segment (24 aa) that was used for NMR measurements are in red.

The growth rate of the yeast strain carrying all five mutated versions of ATP7B matches the yeast strain without ATP7B (Figure 18). This demonstrates that this strain lacks functional Cu transport and prevails as a high-affinity iron-uptake deficient. Reduced growth rates were observed for all the yeast strains carrying the ATP7B variant in which all histidine or all methionine residues were mutated. This shows that Cu transport in these strains is less functional but not completely inhibited. This result clearly indicates that both methionine and histidine residues are responsible for Cu transport. When only one methionine (M682 site) was replaced, no effect on the growth was observed and was similar to that of wildtype ATP7B growth, indicating that this variant was able to transport Cu to Fet3. Notably, replacing all methionine residues had more reduction in growth rate when compared to replacing all histidine in the loop. This implies methionine residues in the loop are more important than histidine residues. Another interesting observation is that when the growth rate differences between M3A and H2A compared to that of yeast without ATP7B *(Δccc2Δatx1* yeast) are summed up, it equals the decreased growth effect of M3H2A variant. This suggests that the reduced growth rate observed in the M3A and H2A variant is the effect of loss of histidine or methionine residues in ATP7B mediated Cu transport. The western blotting analysis confirmed that the expression levels of these variants in yeast were similar to that of ATP7B wildtype. From the results, it can be concluded that most of the methionine and histidine residues present in the luminal loop in ATP7B are required for Cu transport.

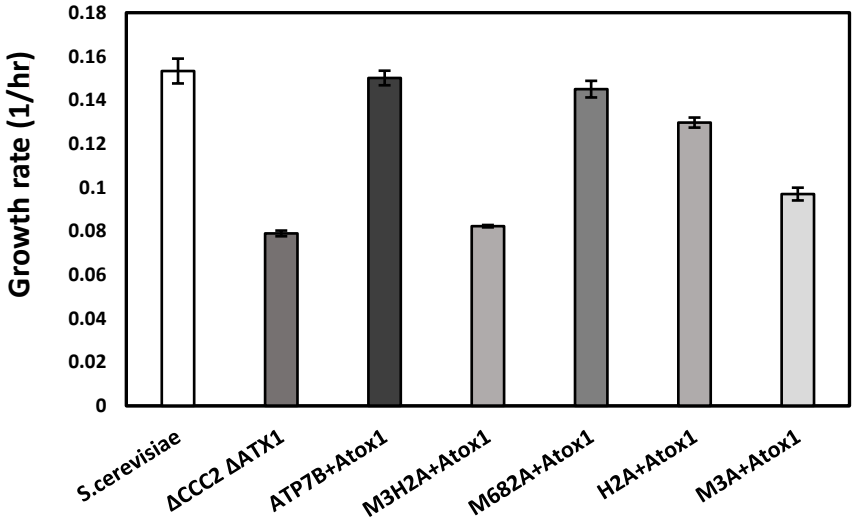


**Figure 18:** Luminal loop mutants in Δ*ccc2*Δ*atx1* yeast. Growth rate of the Δ*ccc2*Δ*atx1* yeast strain complemented with high-copy plasmids with wild-type Atox1 and luminal loop ATP7B variants in iron-limited conditions. Error bars are based on the calculation of weighted errors from six biological replicates.

### 4.6 Localization of ATP7B and its variants

The localization of ATP7B variants (studied for luminal loop mutated ATP7B variants) in yeast cells were visualized via immunofluorescence. Localization of all ATP7B variants were similar like to those observed for cells with wildtype ATP7B (Figure 19). Moreover, all expressed proteins were distributed throughout the yeast cells in a dispersed pattern. This signifies that all ATP7B variant proteins are expressed efficiently in yeast cells and do not agglomerate due to protein misfolding in any specific compartment i.e. in endoplasmic reticulum. Thus the introduced mutations in the luminal loop did not affect the biosynthesis (expression, folding and distribution) of full-length ATP7B. Taken together, western blot and immunostaining results clearly demonstrate that changes in yeast growth rates originate from the defects of ATP7B and not from the low expression levels or localization defects.

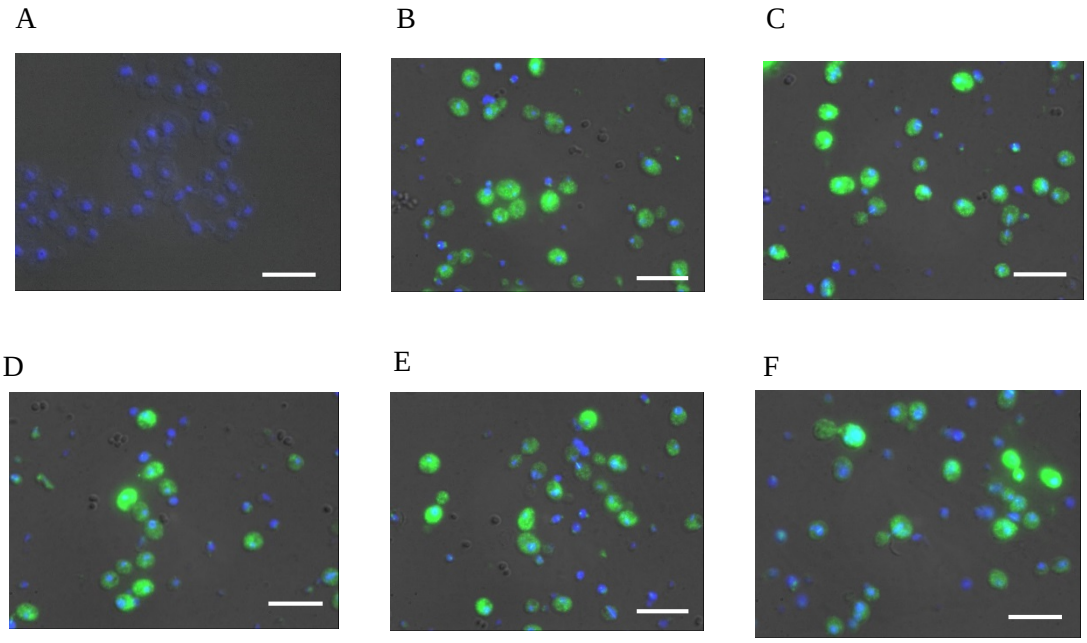


**Figure 19:** Immunostaining of ATP7B variants in yeast cells using a ATP7B-specific antibody. All nuclei were visualized by DAPI staining. **A**. Δ*ccc2*Δ*atx1* yeast without any ATP7B plasmid as control, **B**. Δ*ccc2*Δ*atx1* yeast with wild type ATP7B high-copy plasmid, **C**. Δ*ccc2*Δ*atx1* yeast with H2A ATP7B variant, **D**. Δ*ccc2*Δ*atx1* yeast with M3A ATP7B variant, **E**. Δ*ccc2*Δ*atx1* yeast with M682A variant, and **F**. Δ*ccc2*Δ*atx1* yeast with M3H2A ATP7B variant. Scale bars, 10 µm.

### 4.7 Complementary results (*In-silico* MD and *In vitro* NMR studies on luminal loop of ATP7B)

#### *In-silico* prediction of Cu(I) binding sites in lumen peptide

An *in-silico* luminal peptide model was built with connecting trans-membrane helices and a part of the membrane segment (Figure 17). The loop peptide was predicted to have a disordered structure with a position that protrudes from the membrane.

The histidine and methionine residues in the luminal segment of ATP7B are as follows; H679, H686 and M668, M671, M682. During a 150 ns molecular dynamics simulation, this peptide remained with a disordered structure. The covariance matrix together with principal component analysis (PCA) was used to identify dominating conformational ensembles that were populated during the simulation. Three major conformational states (or clusters) arose when the simulation data was projected along the largest eigenvector-eigenvalue pairs (Figure 20A). Cluster I which comprises of M668, M671 and H679 residues (all three residues are close to each other), appeared during first 18 ns. After 10 ns simulations, they gave rise to a Cluster II which consist of M671, H679 and M682 residues. Last 122 ns displayed Cluster III comprising of M668, M671 and M682 residues (Figure 20B). The computation data presents that the putative Cu(I) binding sites in the luminal peptide involving histidine and methionine residues are partially populated already in the absence of metal. The pre-population of ligand bound structures prior to ligand

binding is called conformational selection mechanism and was found to be compatible with ligand binding to many enzymes.

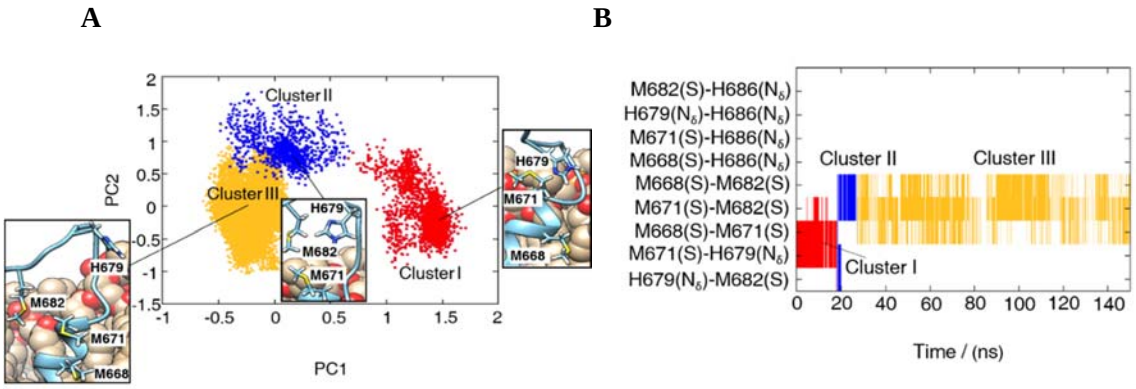


**Figure 20:** Homology model of luminal loop of ATP7B (**A**) The principal component analysis of the WT ATP7B$^{654-710}$ domain. The 150 ns MD trajectories are projected on the two most significant principal components of the first lumen-protruding loop Cα atoms' covariance matrix. The first component corresponds to the x-axis, and the second corresponds to the y-axis. All snapshots are grouped into three clusters: Cluster I (red), Cluster II (blue) and Cluster III (yellow). A relevant structure from each cluster is shown with a cartoon showing residues Met/His in stick and DPPC molecules in sphere. (**B**) Distances among two His (H679 and H686) residues' $N_\delta$ atoms and three Met (M668, M671 and M682) residues' S atoms along the simulation time. All distance values were larger than 0.3 nm. The distance values < 0.6 nm are displayed as lines with different colors corresponding to the individual cluster: Cluster I in red, Cluster II in blue, and Cluster III in yellow.

**NMR spectroscopic studies of the luminal loop in ATP7B**

The luminal loop peptide (synthesized) contains three methionine and two histidine sites which are referred as M2, M5, M16 and H13, H20. The peptides are denoted as L-WT (Luminal Wildtype), L-M3A (substitution of all three methionines (M668, M671 & M682) to alanines), L-H2A (substitution of two histidines (H679 & H686) to Ala) and L-M3H2A (comprising of all histidine and methionine mutations) (Figure 21).

| | |
|---|---|
| L-WT | LMIYMLIPSNEPHQSMVLDHNIIP |
| L-M3A | LAIYALIPSNEPHQSAVLDHNIIP |
| L-H2A | LMIYMLIPSNEPAQSMVLDANIIP |
| L-M3H2A | LAIYALIPSNEPAQSAVLDANIIP |

**Figure 21:** Primary sequences used in NMR experiments (with KK added to the N-terminus of all constructs to increase solubility, making each peptide 26 residues long).

**Luminal loop peptide is unstructured in solution**

The one-dimensional proton NMR spectroscopic data shows that the luminal loop peptide (L-WT) is unstructured (also supported by far-UV CD data) (Figure 22A). The chemical shifts arising from aromatic acids and several side chains resonances are shown in Figure 22B. The detected signals in this spectral range are notably derived from Y4, H13, H20 and N21 residues in the peptide. This spectral range is focused for the following Cu-luminal loop peptide interaction studies. The acquisition of a two-dimensional 1H-13C HSQC spectrum increased the spectral resolution and provided significant support to the assignment of proton resonance signals.

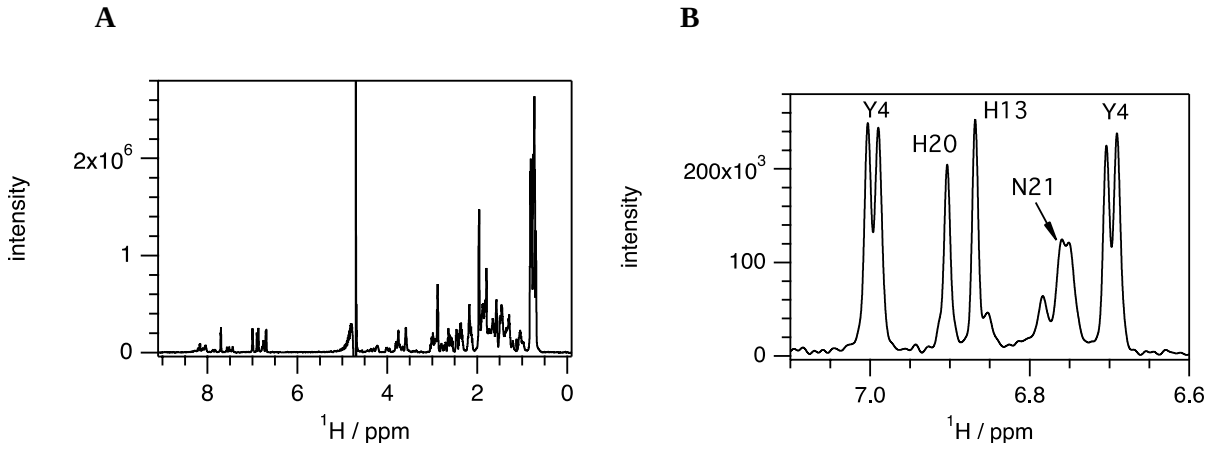


**Figure 22:** One-dimensional proton NMR spectra for L-WT peptide. (**A**) Chemical shifts for all protons of the wild type peptide. (**B**) Chemical shifts of the selected aromatic and side chain resonances only. Associated assignment is shown by using the one letter code for amino acids following position in primary sequence.

When compared to L-WT, the L-H2A and L-M3A peptides had minor changes in the chemical shift pattern whereas L-M3H2A peptide (Figure 24) had slightly more changes than the L-H2A or L-M3A peptide, but overall the mutated peptides retain the structural characteristics of L-WT.

**Interaction of luminal loop peptide with copper**

Interaction of Cu(II) with the L-WT peptide (1:1 Cu(II):peptide) had significant changes in chemical shift pattern observed by an increase in linewidth of peptide resonances. Furthermore, the L-WT peptide tends to precipitate when Cu (II) is added. Cu(I) interaction with L-WT peptide (1:1 Cu:peptide) showed profound changes in the chemical shift pattern noticed by decrease in H13 and loss of H20 signals (Figure 23). Further, addition of Cu(I) (2:1 Cu: peptide) amplified the changes in the chemical shift observed during 1:1 Cu-peptide, and in addition had a slight change in Y4 signal (next to putative Cu ligand M5). This suggests there is more than one Cu(I) binding site in L-WT peptide.

As a next step, the diffusion coefficient are determined from NMR diffusion spectra. Both apo-L-WT and Cu(I) bound peptide had a diffusion coefficient of 1.45 x $10^{-10}$ $m^2S^{-1}$ that corresponds to the hydrodynamic radius of 16.7Å. For a random 26 aa unstructured monomeric peptide the calculated hydrodynamic radius is 14Å and for a trimeric peptide is 26Å. This indicates that the unstructured L-WT

peptide is monomeric in solution both in the presence and absence of Cu(I). Thus, L-WT peptide had at least two Cu(I) binding site while remaining monomeric state in a solution and display Cu(I) affinity in the micromolar concentration range.

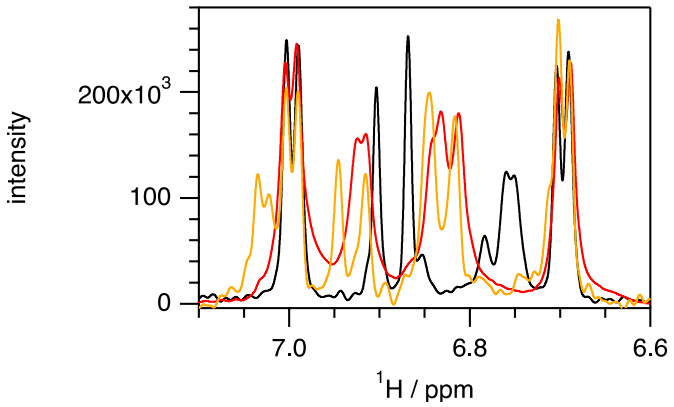


**Figure 23:** Interaction of Cu(I) with luminal loop peptide. One-dimensional proton NMR spectra for L-WT (refer to figure 22B) in absence (black) and in presence of one Cu(I) ion (red) or two Cu(I) ions per peptide (orange), respectively.

Addition of Cu(I) to L-H2A or L-M3A peptide induced site-specific changes in the chemical shift pattern and increasing the Cu(I) amounts (2:1) showed no significant change in the chemical shift pattern which implies both peptides have only one Cu(I) binding site (affinity in the low micromolar concentration). The diffusion coefficient determined for L-H2A and L-M3A peptide provides evidence that the peptides remain in the same monomeric state when it is bound to Cu(I).

The chemical shift pattern of L-M3H2A peptide did not change in addition of Cu(I) which suggest that L-M3H2A peptide does not bind Cu(I) (Figure 24). Further, it implies that the some of histidine and methionine residues in the L-WT peptide are needed for Cu(I) binding. Moreover, the results obtained from the *in vitro* NMR spectroscopy matches with the *in vivo* yeast results which showcase that combination of histidine and methionine residues are essential for Cu(I) binding in the segment of the luminal loop.

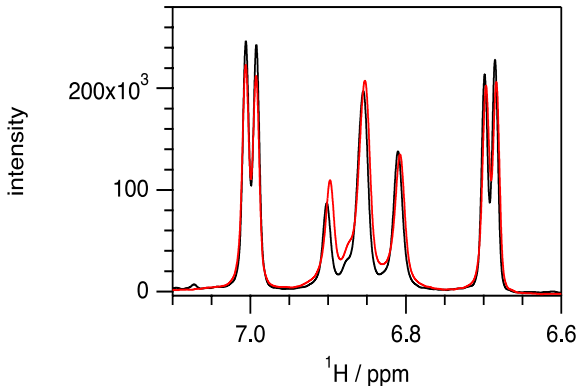


**Figure 24:** Interaction of Cu(I) with L-M3H2A peptide. One-dimensional proton NMR spectra of L-WT peptide and the L-M3H2A variant. Replacing of all histidine and methionine residues with alanine residues induces changes in the chemical shift pattern L-M3H2A (black). Note that chemical shift values and signal

width are almost as seen for the aromatic protons of Y4 (Fig. 22B) are fully retained. The addition of one Cu(I) to L-M3H2A (red) did not change the chemical shift pattern compared to the absence of Cu(I) (black).

Though there may be differences between the *invitro* studies using only the luminal loop segment as a peptide, and the *in vivo* expression of the full length ATP7B protein and its variants, several implications can be made from the results obtained from NMR spectroscopy when combined with the results from full-length ATP7B (yeast assays).

Notably, replacing all histidine and methionine residues in the luminal loop peptide abolishes Cu(I) binding which is in accordance with the results obtained from the *in vivo* studies in yeast where we expressed the full-length ATP7B with corresponding mutations. Inability of M3H2A (all five mutations) variant of ATP7B to transport Cu in yeast is due to the abolished Cu(I) binding in the luminal loop peptide. The Cu transport efficiency of H2A and M3A variants in yeast is less than in the wildtype ATP7B but the NMR spectroscopic data show that the L-H2A and L-M3A peptide binds one Cu(I) ions which implies that specific Cu (I) binding sites or the number of Cu(I) ions that binds simultaneously are vital for the ATP7B function. Taken all together, it appears that the Cu(I) binding sites require a combination of histidine and methionine residues and more than one Cu(I) binding sites are present in the luminal loop. This conclusion is also supported by the real time data obtained from computational MD simulations in absence of Cu, which showed partially populated Cu-binding sites of the luminal loop segment with histidine and methionine residues (cluster I and II).

A study showed the presence of two distinct Cu binding sites in ATP7A which is constituted by a combination of histidine and methionine residues, in accordance with our findings for ATP7B. Mutation on the Cu binding residues in ATP7A resulted in the inhibition of dephosphorylation and Cu-release functions [14]. Previous work on Cu binding sites in transmembrane was suggested to include three sequential Cu binding sites noticeably, a Cu entry site which involves charged residues, central Cu binding site involving conserved CPC motif (ion transduction) and Cu release site which involves D765 residue and plus four nearby methionine residues[115]. In our homology model, we highlight a final Cu exit site in the luminal loop segment of ATP7B involving combination of histidine and methionine residues. This Cu exit site adds to the previous three Cu sites in transmembrane. This finding is supported by our results *in vivo*, as well as the, *in vitro* NMR study and the *in silico* computational MD simulations.

In paper II, we analyzed the luminal loop segment of the ATP7B using the established yeast model where we expressed the full protein with relevant mutations, and *in vitro* NMR and *in silico* computational MD, both focused on the luminal loop segment. The results obtained from this study validates that the luminal segment of ATP7B can bind Cu(I) using histidine and methionine residues in this region. Thus, ATP7B appears to have a copper exit site in the luminal loop segment, similar to ATP7A.

To summarize, the developed yeast model system proved to be an efficient tool to analyze the functional roles of MBDs and the luminal loop of ATP7B in Cu transport activity. Presence of at least one N-terminal MBD in ATP7B is required for receiving Cu from Atox1. The luminal protruding loop that links transmembrane helices TMD1 and TMD2 binds Cu(I) using specific methionine and histidine residue (M668,M671,M682,H679, and H686).

## 5. CONCLUDING REMARKS AND OUTLOOK

Copper and iron metabolism are intertwined in eukaryotic organisms and their disorders are implicated in increasing number of diseases. Understanding the mechanism of Cu and Fe homeostasis is a prerequisite to study human diseases. Wilson's disease is a genetic disorder that affects Cu-transport due to the abnormal functioning of ATP7B protein which is responsible for regulating *in vivo* Cu levels primarily in liver cells. The functional role of ATP7B is extensively studied to explore the underlying processes leading to the Cu toxicity. In those studies, yeast is the preferred model organism to understand the role of Cu ATPase function since the Cu transport proteins and pathways are highly conserved from yeast to humans [102].

Among all types of yeast, the baker's (budding) yeast (*S. cerevisiae*) is widely used as a model organism to establish the mechanisms related to human diseases. This is simply due to its well characterized Cu transport pathway. The application of yeast complementation assay for the study of Cu-ATPases provides us a sensitive tool to assess the putative Cu transporting function of various mutants. This functional assay has been extensively used to study human Cu-ATPase ATP7A & ATP7B and previously used as a diagnostic tool for WD [100, 101]. In this functional assay, the mutant proteins are evaluated only by their relative ability to complement yeast mutants (i.e. how much copper transport activity is required for yeast survival) and not by the exact change in protein activity. However, the yeast complementation assay is an effective way to identify ATP7B mutants, which totally diminished transport activity to those that have very low activity. Other Cu-transport assays typically requires the usage of radioactive Cu ($^{64}$Cu) isotope which has a short half-life (12.7 hours) and are difficult to work. This need can be eliminated with the employment of yeast complementation assay.

Earlier studies using yeast assays have provided significant information about the disease-causing mutations in ATP7B, the importance of metal binding domains, phosphorylation, and ATP binding site and Cu binding regions of ATP7B. All of these studies have been carried out in Δ*ccc2* yeast strain in absence of Atox1. In order to acquire detailed information about Atox1-ATP7B interactions and also to determine which MBD of ATP7B receives Cu from Atox1, we performed experiments using Δ*ccc2*Δ*atx1* yeast strain which were complemented with ATP7B and Atox1. Δ*ccc2*Δ*atx1* yeast strain lack native intracellular Cu transporter Ccc2 and Atx1. Incorporation of ATP7B and Atox1 proteins in this strain has enabled transport of Cu to Fet3 in iron-limited medium. This yeast model system is similar to the intracellular human Cu transport and helps us in understanding the human Cu transport proteins. The combination of new yeast

system and complementation assay will be a valuable tool to explore the interactions of other Cu transport proteins. Till date, the genotype-phenotype correlation in WD has not been established, and due to this, treatment of WD patients is delayed. Inclusion of yeast phenotypic parameters could help to establish genotype-phenotype correlations in WD and provide further mechanistic insights into copper related disorders.

An advantage of this system is that many ATP7B mutant variants can be analyzed in a short time. In our work we used the model to unravel the essential role of MBDs and luminal loop of ATP7B. Presence of at least one cytosolic N-terminal metal binding domain is required to transport Cu along ATP7B (Paper 1). Removal of MBDs hinders ATP7B mediated Cu transport in our yeast system. ATP7B mediated Cu transport involves several intricate intramolecular interactions that are not known yet, and these interactions are important for movement of Cu through ATP7B. Previous research has provided evidence on the interactions of MBDs in ATP7B [84]. Certainly, interactions between MBDs are also crucial for the movement of Cu across ATP7B. There are numerous studies on the cytosolic and transmembrane domains in ATP7B but less attention is given towards the luminal section of ATP7B. In this thesis, apart from MBDs we also focused on the luminal section of ATP7B that links TMD1 and TMD2 and has putative Cu(I) binding residues. In our yeast system, we investigated the luminal loop Cu(I) binding residues in ATP7B mediated Cu transport (Paper II). Additionally, *in vitro* NMR spectroscopic studies were carried out on the luminal loop model peptide to examine Cu(I)-peptide interactions, and *in-silico* molecular dynamic studies was performed to determine the putative Cu(I) binding sites. The results obtained from *in vitro* NMR experiments confirmed that ATP7B bind Cu(I) using histidine (H679, H686) and methionine (M668, M671, M682) residues, found in this region. Combined results from these methods imply that ATP7B has a Cu exit site in the lumen segment. The methods established in this work could further be used to probe the Cu transport function in Wilson's disease-causing ATP7B variants, the role of Atox1 mutants in Cu transport and to investigate the Cu transport function of different Cu ATPases. It may also be possible to exploit the yeast model system to characterize more in depth the physiology and phenotypes of mutant variants and study mitochondrial damage, oxidative damage, or lipid metabolism, all of which have all been observed in WD patients. Ultimately, one could aim to establish a mechanistic model (using yeast) to determine how copper transport and homeostasis dysregulation is connected to metabolism.

To conclude, the developed yeast model system provides information about the functional role of metal binding domains and the luminal loop of ATP7B and shows great potential for investigating human Cu transport in greater detail. In the future, this yeast model system could serve as a useful platform for studying disorders that relates to imbalances in copper homeostasis.

## 6. ACKNOWLEDGEMENTS

I would like to express my gratitude to the following people:

First, my supervisor, **Pernilla Wittung-Stafshede** for all your guidance and support: Thank you so much for sharing your knowledge and experience with me.

My co-supervisor, **Dina Petranovic**, for your valuable advice and suggestions. I sincerely thank you for your support.

**Stefan Hohmann**, thank you for being my examiner. I appreciate it very much.

**Xin Chen** for teaching me about molecular biology techniques. Thanks for your guidance.

Members of Protein Biophysics group;
**Istvan,** I learned a lot of things about protein purifications and it always motivates me to work as you do. **Sandra**, you were available for any discussions and extending your help with the manganese project. Thank you! **Ranjeet Kumar,** thanks for your suggestions, scientific discussions and taking care of my experiments when I was not around. It is nice working with you **Candan Arioz**, we came up with a lot of ideas in our project and thanks for sharing your knowledge. **Stephanie,** thanks for your valuable inputs on experiments. **Tony**, thanks for all the scientific discussions and fun stuff.

**Alexandra** & **Emanuele** for your discussion and sharing your views on experiments. My officemate **Sune** for all chats and laughter.

To all my co-authors for an interesting collaboration.

To all my colleagues at the Division of Chemical biology at BIO and Physical chemistry at KEMI.

Finally, to my parents for your endless support and care.

## 7. REFERENCES


1. Crichton, R., *Chapter 1 - An Overview of the Role of Metals in Biology*, in *Biological Inorganic Chemistry (Third Edition)*, R. Crichton, Editor. 2019, Academic Press. p. 1-18.

2. Dean, K.M., Y. Qin, and A.E. Palmer, *Visualizing metal ions in cells: an overview of analytical techniques, approaches, and probes.* Biochimica et biophysica acta, 2012. **1823**(9): p. 1406-1415.

3. Guengerich, F.P., *Introduction to Metals in Biology 2018: Copper homeostasis and utilization in redox enzymes.* J Biol Chem, 2018. **293**(13): p. 4603-4605.

4. Stern, B.R., et al., *Copper and human health: biochemistry, genetics, and strategies for modeling dose-response relationships.* J Toxicol Environ Health B Crit Rev, 2007. **10**(3): p. 157-222.

5. Park, R.H., et al., *Wilson's disease in Scotland.* Gut, 1991. **32**(12): p. 1541-1545.

6. Nagano, K., et al., *Intracellular distribution of the Wilson's disease gene product (ATPase7B) after in vitro and in vivo exogenous expression in hepatocytes from the LEC rat, an animal model of Wilson's disease.* Hepatology, 1998. **27**(3): p. 799-807.

7. Rodriguez-Castro, K.I., F.J. Hevia-Urrutia, and G.C. Sturniolo, *Wilson's disease: A review of what we have learned.* World J Hepatol, 2015. **7**(29): p. 2859-70.

8. Eisses, J.F. and J.H. Kaplan, *The mechanism of copper uptake mediated by human CTR1: a mutational analysis.* J Biol Chem, 2005. **280**(44): p. 37159-68.

9. Prohaska, J.R., *Role of copper transporters in copper homeostasis.* Am J Clin Nutr, 2008. **88**(3): p. 826s-9s.

10. Morin, I., et al., *Dissecting the role of the N-terminal metal-binding domains in activating the yeast copper ATPase in vivo.* FEBS J, 2009. **276**(16): p. 4483-95.

11. Huster, D., et al., *Diverse Functional Properties of Wilson Disease ATP7B Variants.* Gastroenterology, 2012. **142**(4): p. 947-956.e5.

12. Arioz, C., Y. Li, and P. Wittung-Stafshede, *The six metal binding domains in human copper transporter, ATP7B: molecular biophysics and disease-causing mutations.* Biometals, 2017. **30**(6): p. 823-840.

13. Gonzalez-Guerrero, M. and J.M. Arguello, *Mechanism of Cu+-transporting ATPases: soluble Cu+ chaperones directly transfer Cu+ to transmembrane transport sites.* Proc Natl Acad Sci U S A, 2008. **105**(16): p. 5992-7.

14. Barry, A.N., et al., *The Lumenal Loop Met(672)–Pro(707) of Copper-transporting ATPase ATP7A Binds Metals and Facilitates Copper Release from the Intramembrane Sites.* The Journal of Biological Chemistry, 2011. **286**(30): p. 26585-26594.

15. Yuan, D.S., et al., *The Menkes/Wilson disease gene homologue in yeast provides copper to a ceruloplasmin-like oxidase required for iron uptake.* Proceedings of the National Academy of Sciences of the United States of America, 1995. **92**(7): p. 2632-2636.

16. Brose, J., et al., *Redox sulfur chemistry of the copper chaperone Atox1 is regulated by the enzyme glutaredoxin 1, the reduction potential of the glutathione couple GSSG/2GSH and the availability of Cu(I).* Metallomics, 2014. **6**(4): p. 793-808.

17. Malkin, R. and B.G. Malmstrom, *The state and function of copper in biological systems.* Adv Enzymol Relat Areas Mol Biol, 1970. **33**: p. 177-244.

18. Bost, M., et al., *Dietary copper and human health: Current evidence and unresolved issues.* Journal of Trace Elements in Medicine and Biology, 2016. **35**: p. 107-115.

19. Irving, H. and R.J.P. Williams, *Order of Stability of Metal Complexes.* Nature, 1948. **162**: p. 746.

20. Festa, R.A. and D.J. Thiele, *Copper: An essential metal in biology.* Current Biology, 2011. **21**(21): p. R877-R883.

21. Bremner, I., *Manifestations of copper excess.* Am J Clin Nutr, 1998. **67**(5 Suppl): p. 1069s-1073s.

22. Hasan, N.M. and S. Lutsenko, *Chapter Six - Regulation of Copper Transporters in Human Cells*, in *Current Topics in Membranes*, J.M. Argüello and S. Lutsenko, Editors. 2012, Academic Press. p. 137-161.

23. Linder, M.C., et al., *Copper transport.* Am J Clin Nutr, 1998. **67**(5 Suppl): p. 965s-971s.

24. Fanni, D., et al., *Expression of ATP7B in normal human liver.* Eur J Histochem, 2005. **49**(4): p. 371-8.

25. Ferapontova, E.E., et al., *Direct Electrochemistry of Proteins and Enzymes*, in *Perspectives in Bioanalysis*, E. Paleček, F. Scheller, and J. Wang, Editors. 2005, Elsevier. p. 517-598.

26. Balamurugan, K. and W. Schaffner, *Copper homeostasis in eukaryotes: Teetering on a tightrope.* Biochimica et Biophysica Acta (BBA) - Molecular Cell Research, 2006. **1763**(7): p. 737-746.

27. Zhang, B., et al., *Activity of Metal-Responsive Transcription Factor 1 by Toxic Heavy Metals and H(2)O(2) In Vitro Is Modulated by Metallothionein.* Molecular and Cellular Biology, 2003. **23**(23): p. 8471-8485.

28. Cherukuri, S., et al., *Unexpected role of ceruloplasmin in intestinal iron absorption.* Cell Metab, 2005. **2**(5): p. 309-19.

29. Pena, M.M., S. Puig, and D.J. Thiele, *Characterization of the Saccharomyces cerevisiae high affinity copper transporter Ctr3.* J Biol Chem, 2000. **275**(43): p. 33244-51.

30. Labbe, S., Z. Zhu, and D.J. Thiele, *Copper-specific transcriptional repression of yeast genes encoding critical components in the copper transport pathway.* J Biol Chem, 1997. **272**(25): p. 15951-8.

31. Rees, E.M. and D.J. Thiele, *Identification of a vacuole-associated metalloreductase and its role in Ctr2-mediated intracellular copper mobilization.* J Biol Chem, 2007. **282**(30): p. 21629-38.

32. Hassett, R.F., A.M. Romeo, and D.J. Kosman, *Regulation of high affinity iron uptake in the yeast Saccharomyces cerevisiae. Role of dioxygen and Fe.* J Biol Chem, 1998. **273**(13): p. 7628-36.

33. Stearman, R., et al., *A permease-oxidase complex involved in high-affinity iron uptake in yeast.* Science, 1996. **271**(5255): p. 1552-7.

34. Lutsenko, S., et al., *Function and regulation of human copper-transporting ATPases.* Physiol Rev, 2007. **87**(3): p. 1011-46.

35. Terada, K., et al., *ATP7B (WND) protein.* The International Journal of Biochemistry & Cell Biology, 1998. **30**(10): p. 1063-1067.

36. Chandhok, G., et al., *Functional analysis and drug response to zinc and D-penicillamine in stable ATP7B mutant hepatic cell lines.* World J Gastroenterol, 2016. **22**(16): p. 4109-19.

37. Harada, M., et al., *A mutation of the Wilson disease protein, ATP7B, is degraded in the proteasomes and forms protein aggregates.* Gastroenterology, 2001. **120**(4): p. 967-74.

38. Forbes, J.R., G. Hsi, and D.W. Cox, *Role of the copper-binding domain in the copper transport function of ATP7B, the P-type ATPase defective in Wilson disease.* J Biol Chem, 1999. **274**(18): p. 12408-13.

39. Hedera, P., *Update on the clinical management of Wilson's disease.* The Application of Clinical Genetics, 2017. **10**: p. 9-19.

40. Tümer, Z. and L.B. Møller, *Menkes disease.* European Journal Of Human Genetics, 2009. **18**: p. 511.

41. Ojha, R. and A.N. Prasad, *Menkes disease: what a multidisciplinary approach can do.* J Multidiscip Healthc, 2016. **9**: p. 371-85.

42. Sedlák, E., G. Žoldák, and P. Wittung-Stafshede, *Role of Copper in Thermal Stability of Human Ceruloplasmin.* Biophysical Journal, 2008. **94**(4): p. 1384-1391.

43. Gitlin, J.D., et al., *Mechanisms of caeruloplasmin biosynthesis in normal and copper-deficient rats.* Biochem J, 1992. **282 ( Pt 3)**: p. 835-9.

44. Harris, Z.L., *Aceruloplasminemia.* J Neurol Sci, 2003. **207**(1-2): p. 108-9.

45. Roberti Mdo, R., et al., *Aceruloplasminemia: a rare disease - diagnosis and treatment of two cases.* Rev Bras Hematol Hemoter, 2011. **33**(5): p. 389-92.

46. Waggoner, D.J., T.B. Bartnikas, and J.D. Gitlin, *The role of copper in neurodegenerative disease.* Neurobiol Dis, 1999. **6**(4): p. 221-30.

47. Van Damme, P., W. Robberecht, and L. Van Den Bosch, *Modelling amyotrophic lateral sclerosis: progress and possibilities.* Disease Models & Mechanisms, 2017. **10**(5): p. 537.

48. Ghasemi, M. and R.H. Brown, Jr., *Genetics of Amyotrophic Lateral Sclerosis.* Cold Spring Harb Perspect Med, 2018. **8**(5).

49. Desai, V. and S.G. Kaler, *Role of copper in human neurological disorders.* The American Journal of Clinical Nutrition, 2008. **88**(3): p. 855S-858S.

50. Tokuda, E. and Y. Furukawa, *Copper Homeostasis as a Therapeutic Target in Amyotrophic Lateral Sclerosis with SOD1 Mutations.* Int J Mol Sci, 2016. **17**(5).

51. Price, D.L. and S.S. Sisodia, *Mutant genes in familial Alzheimer's disease and transgenic models.* Annu Rev Neurosci, 1998. **21**: p. 479-505.

52. Atwood, C.S., et al., *Dramatic aggregation of Alzheimer abeta by Cu(II) is induced by conditions representing physiological acidosis.* J Biol Chem, 1998. **273**(21): p. 12817-26.

53. Multhaup, G., et al., *Copper-binding amyloid precursor protein undergoes a site-specific fragmentation in the reduction of hydrogen peroxide.* Biochemistry, 1998. **37**(20): p. 7224-30.

54. Selkoe, D.J., *The cell biology of beta-amyloid precursor protein and presenilin in Alzheimer's disease.* Trends Cell Biol, 1998. **8**(11): p. 447-53.

55. Giampietro, R., et al., *The Pivotal Role of Copper in Neurodegeneration: A New Strategy for the Therapy of Neurodegenerative Disorders.* Mol Pharm, 2018. **15**(3): p. 808-820.

56. Castillo-Gonzalez, J.A., et al., *Phosphorylated α-Synuclein-Copper Complex Formation in the Pathogenesis of Parkinson's Disease.* Parkinson's Disease, 2017. **2017**: p. 9164754.

57. Villar-Pique, A., et al., *Copper(II) and the pathological H50Q alpha-synuclein mutant: Environment meets genetics.* Commun Integr Biol, 2017. **10**(1): p. e1270484.

58. Carboni, E. and P. Lingor, *Insights on the interaction of alpha-synuclein and metals in the pathophysiology of Parkinson's disease.* Metallomics, 2015. **7**(3): p. 395-404.

59. Stockel, J., et al., *Prion protein selectively binds copper(II) ions.* Biochemistry, 1998. **37**(20): p. 7185-93.

60. Stella, G.M., et al., *Cancers of unknown primary origin: current perspectives and future therapeutic strategies.* Journal of Translational Medicine, 2012. **10**: p. 12-12.

61. Wang, F., et al., *Turning Tumor-Promoting Copper into an Anti-Cancer Weapon via High-Throughput Chemistry.* Current medicinal chemistry, 2010. **17**(25): p. 2685-2698.

62. Khan, G. and S. Merajver, *Copper chelation in cancer therapy using tetrathiomolybdate: an evolving paradigm.* Expert Opin Investig Drugs, 2009. **18**(4): p. 541-8.

63. Garber, K., *Cancer's copper connections.* Science, 2015. **349**(6244): p. 129.

64. Itoh, S., et al., *Novel role of antioxidant-1 (Atox1) as a copper-dependent transcription factor involved in cell proliferation.* J Biol Chem, 2008. **283**(14): p. 9157-67.

65. Huffman, D.L. and T.V. O'Halloran, *Function, structure, and mechanism of intracellular copper trafficking proteins.* Annu Rev Biochem, 2001. **70**: p. 677-701.

66. Hussain, F. and P. Wittung-Stafshede, *Impact of cofactor on stability of bacterial (CopZ) and human (Atox1) copper chaperones.* Biochim Biophys Acta, 2007. **1774**(10): p. 1316-22.

67. Niemiec, M.S., C.F. Weise, and P. Wittung-Stafshede, *In vitro thermodynamic dissection of human copper transfer from chaperone to target protein.* PLoS One, 2012. **7**(5): p. e36102.

68. Harrison, M.D., et al., *Intracellular copper routing: the role of copper chaperones.* Trends in Biochemical Sciences, 2000. **25**(1): p. 29-32.

69. Flores, A.G. and V.M. Unger, *Atox1 contains positive residues that mediate membrane association and aid subsequent copper loading.* J Membr Biol, 2013. **246**(12): p. 903-13.

70. Portnoy, M.E., et al., *Structure-function analyses of the ATX1 metallochaperone.* J Biol Chem, 1999. **274**(21): p. 15041-5.

71. Hamza, I., et al., *The metallochaperone Atox1 plays a critical role in perinatal copper homeostasis.* Proc Natl Acad Sci U S A, 2001. **98**(12): p. 6848-52.

72. Palmgren, M.G. and P. Nissen, *P-Type ATPases.* Annual Review of Biophysics, 2011. **40**(1): p. 243-266.

73. Solioz, M. and C. Vulpe, *CPx-type ATPases: a class of P-type ATPases that pump heavy metals.* Trends Biochem Sci, 1996. **21**(7): p. 237-41.

74. Sebastian, T.T., et al., *Phospholipid flippases: building asymmetric membranes and transport vesicles.* Biochimica et Biophysica Acta, 2012. **1821**(8): p. 1068-1077.

75. Stokes, D.L. and N.M. Green, *Structure and function of the calcium pump.* Annu Rev Biophys Biomol Struct, 2003. **32**: p. 445-68.

76. Bunce, J., et al., *Copper transfer studies between the N-terminal copper binding domains one and four of human Wilson protein.* Biochim Biophys Acta, 2006. **1760**(6): p. 907-12.

77. Patil, M., et al., *A Review and Current Perspective on Wilson Disease.* Journal of Clinical and Experimental Hepatology, 2013. **3**(4): p. 321-336.

78. Polishchuk, Elena V., et al., *Wilson Disease Protein ATP7B Utilizes Lysosomal Exocytosis to Maintain Copper Homeostasis.* Developmental Cell, 2014. **29**(6): p. 686-700.

79. Yang, X.L., et al., *Two forms of Wilson disease protein produced by alternative splicing are localized in distinct cellular compartments.* Biochem J, 1997. **326 ( Pt 3)**: p. 897-902.

80. Banci, L., et al., *Metal binding domains 3 and 4 of the Wilson disease protein: solution structure and interaction with the copper(I) chaperone HAH1.* Biochemistry, 2008. **47**(28): p. 7423-9.

81. Andersson, M., et al., *Copper-transporting P-type ATPases use a unique ion-release pathway.* Nat Struct Mol Biol, 2014. **21**(1): p. 43-8.

82. Jayakanthan, S., et al., *Human copper transporter ATP7B (Wilson disease protein) forms stable dimers in vitro and in cells.* J Biol Chem, 2017. **292**(46): p. 18760-18774.

83. Nagano, K., et al., *Gene-mediated expression and partial characterization of ATPase 7B in cultured cells.* The Journal of Trace Elements in Experimental Medicine, 1997. **10**(2): p. 111-117.

84. Huang, Y., et al., *Interactions between metal-binding domains modulate intracellular targeting of Cu(I)-ATPase ATP7B, as revealed by nanobody binding.* J Biol Chem, 2014. **289**(47): p. 32682-93.

85. Roelofsen, H., et al., *Copper-induced apical trafficking of ATP7B in polarized hepatoma cells provides a mechanism for biliary copper excretion.* Gastroenterology, 2000. **119**(3): p. 782-93.

86. Roelofsen, H., R. Balgobind, and R.J. Vonk, *Proteomic analyzes of copper metabolism in an in vitro model of Wilson disease using surface enhanced laser desorption/ionization-time of flight-mass spectrometry.* J Cell Biochem, 2004. **93**(4): p. 732-40.

87. Forbes, J.R. and D.W. Cox, *Copper-dependent trafficking of Wilson disease mutant ATP7B proteins.* Hum Mol Genet, 2000. **9**(13): p. 1927-35.

88. van den Berghe, P.V., et al., *Reduced expression of ATP7B affected by Wilson disease-causing mutations is rescued by pharmacological folding chaperones 4-phenylbutyrate and curcumin.* Hepatology, 2009. **50**(6): p. 1783-95.

89. Jain, S., G.G. Farias, and J.S. Bonifacino, *Polarized sorting of the copper transporter ATP7B in neurons mediated by recognition of a dileucine signal by AP-1.* Mol Biol Cell, 2015. **26**(2): p. 218-28.

90. Michalczyk, A., et al., *ATP7B expression in human breast epithelial cells is mediated by lactational hormones.* J Histochem Cytochem, 2008. **56**(4): p. 389-99.

91. Guo, Y., et al., *NH2-terminal signals in ATP7B Cu-ATPase mediate its Cu-dependent anterograde traffic in polarized hepatic cells.* Am J Physiol Gastrointest Liver Physiol, 2005. **289**(5): p. G904-16.

92. Lorinczi, E., et al., *Delivery of the Cu-transporting ATPase ATP7B to the plasma membrane in Xenopus oocytes.* Biochim Biophys Acta, 2008. **1778**(4): p. 896-906.

93. Yatsunyk, L.A. and A.C. Rosenzweig, *Cu(I) binding and transfer by the N terminus of the Wilson disease protein.* J Biol Chem, 2007. **282**(12): p. 8622-31.

94. Huster, D., et al., *Defective cellular localization of mutant ATP7B in Wilson's disease patients and hepatoma cell lines.* Gastroenterology, 2003. **124**(2): p. 335-45.

95. Tsivkovskii, R., B.C. MacArthur, and S. Lutsenko, *The Lys1010-Lys1325 fragment of the Wilson's disease protein binds nucleotides and interacts with the N-terminal domain of this protein in a copper-dependent manner.* J Biol Chem, 2001. **276**(3): p. 2234-42.

96. Bartee, M.Y., M. Ralle, and S. Lutsenko, *The Loop Connecting Metal-Binding Domains 3 and 4 of ATP7B Is a Target of a Kinase-Mediated Phosphorylation.* Biochemistry, 2009. **48**(24): p. 5573-5581.

97. Gupta, A., et al., *Cellular copper levels determine the phenotype of the Arg(875) variant of ATP7B/Wilson disease protein.* Proceedings of the National Academy of Sciences of the United States of America, 2011. **108**(13): p. 5390-5395.

98. Barry, A.N., et al., *The lumenal loop Met672-Pro707 of copper-transporting ATPase ATP7A binds metals and facilitates copper release from the intramembrane sites.* J Biol Chem, 2011. **286**(30): p. 26585-94.

99. Huster, D., et al., *High copper selectively alters lipid metabolism and cell cycle machinery in the mouse model of Wilson disease.* J Biol Chem, 2007. **282**(11): p. 8343-55.

100. Cater, M.A., et al., *Intracellular trafficking of the human Wilson protein: the role of the six N-terminal metal-binding sites.* Biochemical Journal, 2004. **380**(Pt 3): p. 805-813.

101. Papur, O.S., O. Terzioglu, and A. Koc, *Functional characterization of new mutations in Wilson disease gene (ATP7B) using the yeast model.* J Trace Elem Med Biol, 2015. **31**: p. 33-6.

102. De Freitas, J., et al., *Yeast, a model organism for iron and copper metabolism studies.* Biometals, 2003. **16**(1): p. 185-197.

103. Askwith, C., et al., *The FET3 gene of S. cerevisiae encodes a multicopper oxidase required for ferrous iron uptake.* Cell, 1994. **76**(2): p. 403-10.

104. Pinner, E., et al., *Functional complementation of the yeast divalent cation transporter family SMF by NRAMP2, a member of the mammalian natural resistance-associated macrophage protein family.* J Biol Chem, 1997. **272**(46): p. 28933-8.

105. Teem, J.L., et al., *Identification of revertants for the cystic fibrosis delta F508 mutation using STE6-CFTR chimeras in yeast.* Cell, 1993. **73**(2): p. 335-46.

106. Hahn-Hägerdal, B., et al., *Role of cultivation media in the development of yeast strains for large scale industrial use.* Microbial Cell Factories, 2005. **4**: p. 31-31.

107. Froger, A. and J.E. Hall, *Transformation of plasmid DNA into E. coli using the heat shock method.* J Vis Exp, 2007(6): p. 253.

108. Wach, A., et al., *New heterologous modules for classical or PCR-based gene disruptions in Saccharomyces cerevisiae.* Yeast, 1994. **10**(13): p. 1793-808.

109. Steensma, H.Y. and J.J. Ter Linde, *Plasmids with the Cre-recombinase and the dominant nat marker, suitable for use in prototrophic strains of Saccharomyces cerevisiae and Kluyveromyces lactis.* Yeast, 2001. **18**(5): p. 469-72.

110. Ponnandai Shanmugavel, K., D. Petranovic, and P. Wittung-Stafshede, *Probing functional roles of Wilson disease protein (ATP7B) copper-binding domains in yeast.* Metallomics, 2017. **9**(7): p. 981-988.

111. Gietz, R.D. and R.A. Woods, *Yeast Transformation by the LiAc/SS Carrier DNA/PEG Method*, in *Yeast Protocol*, W. Xiao, Editor. 2006, Humana Press: Totowa, NJ. p. 107-120.

112. Collins, J.F., J.R. Prohaska, and M.D. Knutson, *Metabolic crossroads of iron and copper.* Nutr Rev, 2010. **68**(3): p. 133-47.

113. Cooper, S., *15 - The Eukaryotic Division Cycle*, in *Bacterial Growth and Division*, S. Cooper, Editor. 1991, Academic Press: San Diego. p. 389-428.

114. Iida, M., et al., *Analysis of functional domains of Wilson disease protein (ATP7B) in Saccharomyces cerevisiae.* FEBS Lett, 1998. **428**(3): p. 281-5.

115. Schushan, M., et al., *A structural model of the copper ATPase ATP7B to facilitate analysis of Wilson disease-causing mutations and studies of the transport mechanism.* Metallomics, 2012. **4**(7): p. 669-78.